Received: 5 April 2022 | Revised: 7 November 2022 | Accepted: 16 November 2022

DOI: 10.1002/eqe.3787

RESEARCH ARTICLE

WILEY

Numerical study of the seismic retrofitting of masonry-Infilled RC frames with openings using TRM

Filippou Christiana A | **Nicholas C Kyriakides** | **Christis Z Chrysostomou**

Department of Civil Engineering and Geomatics, Cyprus University of Technology, Limassol, Cyprus

Correspondence
Filippou Christiana A., Department of Civil Engineering and Geomatics, Cyprus University of Technology, Achilleos 1 Building, 3rd floor, Office 316 Saripolou 2-8, Limassol 3036, Cyprus.
Email: ca.filippou@edu.cut.ac.cy

Abstract

The seismic retrofitting of existing masonry-infilled reinforced-concrete (RC) frame buildings is one major challenge of earthquake risk mitigation. In this paper, the use of promising novel alternative composite material, namely textile reinforced mortar (TRM) for seismic retrofitting masonry-infilled RC frames with central openings is examined numerically, to the best knowledge of the authors, for the first time ever. This is achieved by performing a parametric study on a validated 2D numerical model of a three-story masonry-infilled RC frame with and without TRM considering different size of central openings. This parametric study aims to examine (i) the influence of central openings on the lateral response of masonry-infilled RC frames subjected to cyclic loading and (ii) the lateral response of the three-story masonry-infilled RC frame with central openings retrofitted with TRM under cyclic loading. From the results obtained in this study, it was concluded that TRM contributes to increase the lateral capacity, stiffness, and the dissipated energy of infilled frames with openings and at the same time provides a more ductile behavior by delaying the strength and the stiffness degradation of infilled frames due to openings and further by delaying or even preventing brittle failures that occur on infilled frames due to the presence of the opening. New stiffness reduction factors for infilled frames with openings, and for TRM-retrofitted infilled frames with openings are also proposed, which can be used with an equivalent compression strut model and with a tension tie-model as an everyday practice tool for simulating infilled frames with central openings along the diagonal of the infill wall with and without TRM. A numerical sensitivity analysis is also performed aiming to investigate the influence of (i) the TRM reinforcement ratio and (ii) the type of mortar used for binding the textile reinforcement on the lateral response of the three-story masonry-infilled RC frame retrofitted with TRM subjected to cyclic loading. This study showed that by increasing the reinforcement ratio, or by using high-strength mortars for binding the textile reinforcement, the lateral capacity of infilled frames is increased leading to a more ductile behavior, but this increase is not proportional to the increase

of the reinforcement ratio or to the increase of the mechanical properties of the mortar.

KEYWORDS
cyclic loading, masonry-infilled RC frames, openings, seismic retrofitting, textile reinforced mortar (TRM)

1 | INTRODUCTION

Reinforced-concrete buildings with masonry-infill walls is the most usual construction typology dispersed globally for commercial, industrial, and family residential use. Most of them have been built before the development of the new seismic regulations rendering them more susceptible to collapse given an earthquake event. Observations from past earthquakes proved the vulnerability of these buildings due to the high degree of damages observed causing casualties and high economic losses. Considering the common construction of masonry-infilled RC frames in several countries, it is of utmost importance to evaluate the seismic performance and to seismic retrofit such type of buildings.

The seismic performance of infilled frames was examined by several researchers since the 1950′s. They concluded that the existence of masonry infill-walls in RC frames increases the lateral capacity of the building and, at the same time it may introduce brittle shear failure mechanisms associated with the infill-frame interaction. The most common failure mechanisms due to irregular distribution of the infill wall in plan and elevation in RC frame are: (a) soft-story mechanism,[1] b) short-column mechanism;[2] and, c) plan torsion effect.[3] Besides the brittle failure mechanisms, most of the researchers reported that five distinct modes of in-plane failure are possible to occur when an infilled frame is subjected to lateral loads, such as: (a) sliding shear, (b) diagonal compression, (c) corner crushing, (d) diagonal cracking, and (e) frame failure mode.[4–9] Adding to this, they concluded that the in-plane lateral response of masonry-infilled RC frames is influenced by several parameters such as the infill-frame relative stiffness and strength, the presence of the openings, the quality of the materials used, and the workmanship, among others. For example, Liauw[10–12] concluded that the presence of connectors at the infill-frame interface increases the stiffness and strength of the infilled frame by about 40–50%. Mehrabi[13] and Mosalam[14] observed that specimens with strong frames and strong infill walls had larger load resistance and dissipated energy than those with weak frames and weak infill. Also, previous studies reported that when strong-frame and weak-infill configuration was used it leads to the shear failure of the columns.[15–19] Experimental studies showed that the mechanical properties of mortar joints influence significantly the failure mode of an infilled frame.[3,14] Regarding the influence of the openings on the lateral response of infilled frames, several experimental and numerical studies have been conducted so far aiming to examine the influence of the openings and their position on the in-plane response of infilled frames under lateral loading.[20–23] Most of them concluded that the presence of an opening in an infilled frame results in a more flexible structural system with lower lateral capacity than the infilled frame without opening, but this decrease is not in proportion to the reduction of the cross-sectional area of the infilled frame due to openings. Mallick and Garg[24] concluded that the loss of strength and stiffness of infilled frames due to a centrally located square opening having dimension one-fifth of the infill wall is ranging from 25% to 50% for both compared to those of infilled frames without opening. Later, Kakaletsis and Karayannis[25–27] pointed out that for openings equal to 12.5% and 25% of the total area of the infill, the decrease of the strength of the infilled frame was equal to 19% and 32%, respectively. Furthermore, previous studies reported that the interaction between the infill wall and frame is adversely affected as the opening position is moved towards the compression diagonal of the infill wall.[28–30] Dawe[31] recommended that the best location for a window or door opening is at the center of the infill wall because if the opening interrupts the compression diagonal it gives an opportunity for two diagonal struts to develop in the infill wall. Asteris et al.[8,32] concluded that the higher value of the stiffness reduction of infilled frames with opening occurs when the opening is upon the diagonal of the infill wall. The authors, among others, proposed an equation for estimating the stiffness of the infill wall as a function of the effective width of the diagonal strut. Moreover, the experimental and numerical studies that have been conducted so far showed that the failures and crack patterns of masonry-infilled RC frames with openings are affected by the location and by the size of the opening, where the cracks are usually developed at the corner of the openings, and as the lateral load increases these cracks propagate towards the loaded corners of infilled frames.[17,23,24] The existence of an opening in masonry-infilled RC frame may create unfavorable failures depending on its location and its size, while the short-column mechanism is very typical for some types of windows, since the infill walls are not continuous through the height of the frame.[35] Besides the research focusing on the in-plane response of infilled frames, several experimental and numerical studies have been also

performed towards the out-of-plane response of infilled frames.[36,37] Some authors reported that the out-of-plane strength of infilled frames decreases with increasing slenderness of the infill wall, while the aspect ratio of the infill wall and the wall boundary conditions directly affect the out-of-plane behavior of the infilled frames.[38,39] Recently, Furtado et al.[40] and Ricci et al.[41] examined the in-plane and out-of-plane interaction behavior of infilled frames. They concluded that the in-plane demands of infilled frames reduce their out-of-plane strength capacity and stiffness.

Despite the several years of research regarding the assessment of the seismic performance of masonry-infilled RC frame buildings, nowadays, their seismic retrofitting is also a challenging engineering problem. Over the years, different retrofitting approaches have been proposed and used so that these buildings can be enhanced to satisfy the modern seismic design codes. However, the existing regulations do not demand any specific rule/recommendation for strengthening of infill walls. The recent retrofitting methods for infilled frames include the use of fiber reinforced polymers (FRP),[42–45] and the use of ductile-fiber-reinforced cementitious composites (FRCM).[46,47] Owing to the need for introducing innovative materials, recently, the Textile Reinforced Mortar (TRM) composite material, which is a combination of inorganic matrix (lime- or cement-based) and non-corrosive multi-axial textile fabrics, has received attention as a sustainable method for retrofitting RC and masonry structures.[48–52] The TRM emerged as the most promising method for retrofitting RC and masonry structures, due to its low-cost price, easy of application, minimal thickness, durability features and compatibility with RC or masonry structures than the widely used ones such as concrete jacketing and FRP. Simultaneously, the use of inorganic matrix as in TRM instead of epoxy resins, as in FRPs, overcomes some of FRP drawbacks such as high cost, incompatibility with substrate materials, and inability to apply on wet surfaces.

While significant research has been conducted so far for retrofitting solid masonry-infilled RC frames, much less has been conducted for masonry walls with openings and for masonry-infilled frames with openings. For example, Benedetti et al.[53] conducted shake table tests on two-story infilled frames with window and door openings in different positions to evaluate the lateral response of existing buildings, and to study the effect of using different retrofitting methods (using cement mixtures for cracks, and steel grids covered with cement layers). The lateral resistance of the retrofitted specimen is increased significantly to that of the original one. Later, tests on large-scale masonry-infilled steel frames with window and door openings retrofitted with high-density polymeric-grids embedded in a mortar layer were conducted by Colombo et al.,[54] and they concluded that the maximum strength of the retrofitted specimen is increased by about 40%-65% compared to that of the unretrofitted one. Several researchers pointed out that the FRP provides an increase of about 50%-300% in the lateral strength, deformation capacity, and in the energy absorption of masonry walls with openings.[55–58] Recently, Proença et al.[59] evaluated experimentally and numerically the in-plane lateral response of masonry walls with openings retrofitted with steel window frame inside the opening. The results showed that the lateral strength and the dissipated energy of the masonry walls with opening is increased by about 40% and 150%, respectively, compared to that of the unretrofitted specimen.

None of either past experimental or numerical studies were geared towards the use of TRM for retrofitting masonry-infilled RC frames with openings, despite that significant research has been conducted for solid masonry-infilled RC frames retrofitted with TRM in the last decade.[32,33,35,44–48,60] In the absence of experimental data, one way of closing this gap of knowledge is to investigate numerically the effectiveness of using the TRM composite material for retrofitting masonry-infilled RC frames with openings, which was the objective of the current study.

Thus, this paper aims to assess the effectiveness of using the TRM to retrofit masonry-infilled RC frame buildings with openings, in order to facilitate the use of TRM as a regular method for retrofitting existing buildings in practical engineering. This is achieved by performing a parametric study on a validated 2D numerical model of a three-story masonry-infilled RC frame with and without TRM considering different size of central openings ranging from 5% to 27%. This parametric study aims to examine (i) the influence of central openings on the lateral response of masonry-infilled RC frames subjected to cyclic loading and (ii) the lateral response of the three-story masonry-infilled RC frame with central openings retrofitted with TRM under cyclic loading. A numerical sensitivity analysis was also performed on the same validated 2D numerical model of the three-story masonry-infilled RC frame with TRM, aiming to investigate the influence of (i) the TRM reinforcement ratio and (ii) the type of mortar used for binding the textile reinforcement on its lateral response. Thus, the major novelties of this research work are: 1) the study of the in-plane seismic response of masonry-infilled RC frame buildings with openings retrofitted with TRM, 2) new stiffness reduction factors for infilled frames with openings, and for TRM-retrofitted infilled frames with openings, which can be used with an equivalent compression strut model and with a tension tie-model as an everyday practice for simulating infilled frames with central openings along the diagonal of the infill wall with and without TRM, and 3) study of the influence of the TRM reinforcement ratio and the type of mortar used for binding the textile reinforcement on the lateral response of the in-plane seismic response of masonry-infilled RC frame buildings.

NOVELTY

- expand the knowledge related to response of infilled frames with central openings
- assess the effectiveness of using TRM for retrofitting infilled frames with openings
- to promote the prospective use of TRM novel material for retrofitting existing infilled frames with and without openings.

2 | BRIEF OVERVIEW OF THE EXPERIMENTAL CASE STUDY

The experimental study used for the calibration of the solid masonry-infilled RC frame model with and without TRM has been carried out by Koutas et al.[49] This study aimed to investigate the effectiveness of using the TRM for retrofitting a 2/3 scale, three-story non-seismically designed masonry-infilled RC frame under in-plane cyclic loading. Two infilled frames were built and tested, with and without TRM. In this section, a short description of this study is presented for the benefit of the reader, while full details about the experimental study can be found in Koutas et al.[49]

The geometry of the masonry-infilled RC frame is given in Figure 1A. For the construction of the RC frame (rectangular columns and T-section beams), C16/20 class of concrete was used (classification based on Eurocode 2[65]), with mean compressive strength and modulus of elasticity equal to 28 MPa and 22 GPa, respectively. The longitudinal ribbed reinforcement had 12 mm diameter and mean yield stress equal to 550 MPa (class of B500C), while smooth steel stirrups with mean value of yield stress equal to 270 MPa (class of S220) were used as transverse reinforcement for all concrete members. The infill wall was constructed from perforated, fired clay bricks. The mean value of the compressive strength of the infill wall was 5.1 MPa, and its modulus of elasticity perpendicular to the bed joints was equal to 3.37 GPa. The diagonal cracking stress (shear strength) of the infill wall ranges from 0.3 to 0.8 MPa, and its mean shear modulus was equal to 1.38 GPa. The infilled frame was supported rigidly by the foundation RC beam plate at the bottom of the frame.

The selection of the TRM retrofitting scheme was dictated by the response of the unretrofitted specimen, especially from the failures that occurred on it. The strengthening scheme is presented in Figure 1B and includes the following: (a) Strengthening the ends of columns at the first and second stories with three (total thickness 9 mm) and two (total thickness 6 mm) layers of carbon-TRM, respectively, fully wrapped around the column to form a closed jacket over a height of 420 mm, (b) Strengthening the two-sides of the infill walls with glass-TRM (externally bonded on the faces of the infill walls) by completely covering vertically the story clear height, and horizontally the area between the extremities of the bounding columns (due to its limited width the textile was applied with an overlap of about 300 mm along the entire length of each bay, near the bottom part of each story), whereas the first story received two layers of TRM (total thickness 12.5 mm)

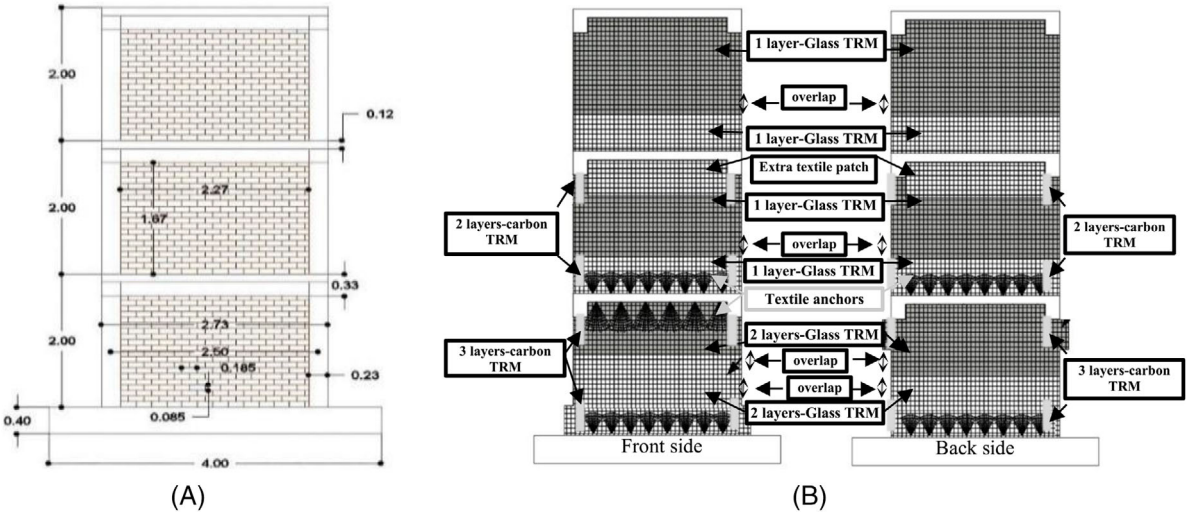

FIGURE 1 (A) Geometry of the masonry-infilled RC frame, and (B) TRM strengthening scheme[49]

and the second and third stories received one layer of TRM (total thickness 7.5 mm) and (c) 11 and 8 textile-based anchors were placed at equal spaces along the infill-beam interfaces, at the first and second story, respectively, where the straight part of the anchor was inserted into predrilled holes filled with injected epoxy resin and the fanned parts was bonded by hand pressure on the top of the first TRM layer. A vertical load of 80 kN per story was applied for both specimens (through prestressing rods), while five and seven cycles of displacement loading were applied to the unretrofitted and retrofitted specimen, respectively. The maximum top-floor displacement for the unretrofitted specimen was equal to 60 mm, which corresponds to 1% top-story drift ratio, and for the retrofitted one was equal to 80 mm, which corresponds to 1.33% top-story drift ratio. The maximum imposed displacement on the two specimens was determined on the basis of achieving at least the conventionally defined failure threshold of 20% drop in the peak load. The experimental results showed that the TRM provides an increase in the lateral strength, deformation capacity and in the dissipated energy of the infilled frame. Specifically, the maximum base-shear of the unretrofitted infilled frame was about ± 250 kN (first story drift ratio equal to 0.77%), and of the retrofitted one was about ± 400 kN (first story drift ratio equal to 1%). Furthermore, the TRM provides a more ductile behavior and contributes to delaying the failures and the cracks that occurred in the infilled frames without retrofitting (diagonal and horizontal cracks along the diagonal of the infill wall, shear cracks at the ends of the columns at the first floor and local crushing of the infill wall near the two upper ends of the columns of the first story). During the last cycles of loading, debonding of TRM from the beam surface and compressive failure of the infill wall at the first story of the retrofitted infilled frame were observed. Knowing that the in-plane and the out-of-plane interaction on infilled frames is a critical parameter influencing the seismic response of infilled frame buildings,[52] in that study, special care was taken to exclude the out-of-plane specimen deformation leaving the in-plane behavior unaffected.

3 | DEVELOPMENT AND VALIDATION OF THE NUMERICAL MODEL OF MASONRY-INFILLED RC FRAME WITH AND WITHOUT TRM

A 2D three-story masonry-infilled RC frame model with and without TRM was developed in DIANA FEA[66] commercial software and validated according to the experimental test conducted by Koutas et al.[49] For the purpose of this study, a 2D simplification is considered although that the complex behavior of masonry-infilled RC frames under lateral loading is a three-dimensional (3D) problem, especially in the case of out-of-plane effects. In this section, a short description of the development and of the validation of the unretrofitted and retrofitted three-story masonry-infilled RC frame model is presented, while more details can be found in Filippou[67] and Filippou et al.[51,68]

The numerical models were developed following a simple micro-modeling approach, and a 2D simplification is considered where the stresses perpendicular to the face of the members are zero (plane-stress elements with a virtual thickness). The concrete members, the masonry infill wall and the TRM are modeled separately by continuum elements (CQ16M quadrilateral isoperimetric plane-stress element) and their geometry is that of the experimental specimens (Figure 1). In this study, the TRM composite is modeled by continuum elements where the textile reinforcement and mortar layer are lumped in a homogenized layer. Figure 2 shows the geometry and the mesh of the masonry-infilled RC frame model with TRM where the shape of elements is kept rectangular with nearly equal size (111 × 115 mm). The infill-frame interface is modeled with a three-point line interface element (CL12I). The CL12I interface element, which is located at the perimeter of the infill wall (between the plane-stress elements of the concrete members and those of the masonry infill wall) has thickness equal to that of the infill wall as shown in Figure 2. The steel reinforcement is modeled with a two-node bar element, and it is connected to the eight-node concrete element (CQ16M) at the two external nodes. In total, 24 two-noded bar elements were used for longitudinal reinforcement with cross sectional area equal to 226.19 mm^2 each, and 172 two-noded bar elements were used for stirrups reinforcement with cross sectional area equal to 56.54 mm^2 each. The location and the cross-sectional area of the reinforcement of each of the two-noded bar reinforcement element in the numerical models is according to that of the experimental specimens. It is important to mention that the textile-based anchors are not modeled, nevertheless, the bond condition provided by the existence of anchors is taken into account in the numerical model as described in Filippou et al.[69,70] All the nodes at the bottom of the unretrofitted and retrofitted infilled frame model are restrained by preventing any translation in the x- and y-direction (Figure 2) to represent the fixed condition between the foundation beam and the infilled frame that was considered in the experiment.

Following the smeared crack approach, four material models are used for describing the non-linear cyclic behavior of the components of this type of structure. Specifically, the Maekawa Fukuura model as a compression function and the *fib* 2010 model as a tension function of the Total Strain Crack model is adopted for the concrete elements. For the steel reinforcement two-noded bar elements the Menegotto-Pinto plasticity model is used. The required parameters of these

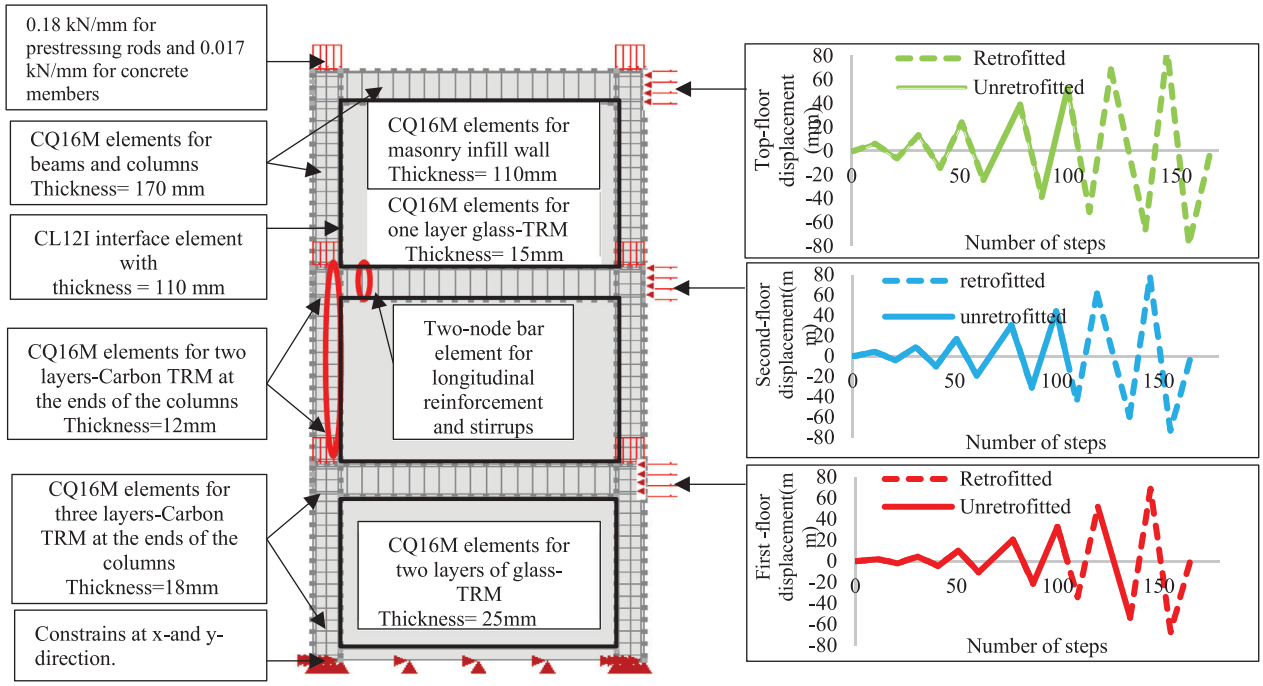

FIGURE 2 Geometry, type of elements, constrains, and loading scheme of the numerical models

TABLE 1 Parameters of the concrete material model and Menegotto-Pinto material model

Maekawa Fukuura model combined with *fib* 2010 model for the Total Strain Crack model		**Menegotto-Pinto model**	
Elastic parameters		**Modulus of elasticity (E)**	**206 GPa**
Modulus of elasticity (E)*	9.1 GPa	Initial yield stress ($\sigma_y{}^0$)	Longitudinal bar :550 MPa Stirrups: 270 MPa
Poison ratio (v)	0.2	Initial tangent slope (b^0)	0.05
Mass density (ρ)	2548 kg/m^3	Initial curvature parameter (R^0)	20
Crack orientation	Rotating	Constant parameter A_1	18.5
Tensile behavior CEB-FIP model code 2010		Constant parameter A_2	0.01
Tensile strength (f_t)	2.15 MPa	Constant parameter A_3	0.2
Fracture energy (G_{ft})	130 N/m	Constant parameter A_4	3
Crack bandwidth specification	Rots		
Compressive behavior: Maekawa concrete model			
Uniaxial compressive strength (f_c)	27.2 MPa		
Damage based tensile strength reduction	Linear		
Confinement model	No increase		

model are presented in Table 1. Furthermore, the Engineering Masonry model is used for the masonry infill wall elements. This model is a smeared crack model available in DIANA FEA that covers the tensile, shear and compression failure of an infill wall and it requires a large number of parameters to be specified as presented in Table 2. Also, the Fiber Reinforced concrete model combined with the *fib* 2010 model are used as a tension and compression softening function, respectively, for the Total Strain Crack model in order to represent the non-linear behavior of the TRM composite material. The required parameters of this model, as given in Table 3, are obtained from the coupon tests conducted by Koutas et al.,[49] and using the analytical model of TRM proposed by Filippou and Chrysostomou.[71] Furthermore, the Coulomb Friction model is adopted for the infill-frame interface elements in order to capture the gap-opening and the sliding between the masonry

TABLE 2 Parameters of the masonry model

Engineering masonry model	
Young modulus (E_y)	3.37 GPa
Young modulus (E_x)	1.62 GPa
Shear modulus ($G_{x,y}$)	1.38 GPa
Cracking behavior: Head joint failure	
Tensile strength normal to the bed joint (f_{ty})	0.5 MPa
Tension fracture energy (G_{ft})	0.05 N/mm
Residual tensile strength (f_{tr})	0.2 MPa
Shear behavior	
Friction angle (φ)	20 °
Cohesion (c)	0.7 MPa
Compressive behavior	
Compressive strength (f_c)	5.1 MPa
Compression fracture energy (G_{fc})	40 N/mm
Factor to strain at compressive strength	1
Unloading factor λ	0.2
Crack band width	
Crack band width specification	Rots

TABLE 3 Parameters of the TRM material model

Fiber reinforced concrete model combined with fib 2010 model for the Total Strain Crack model		
	One-layer Glass–TRM	**Two-layers Glass-TRM**
Elastic modulus (GPa)	30	30.5
Poison ratio	0.2	0.2
Mass density (Kg/m^3)	2400	2400
Tensile behavior	**Fib Fiber Reinforced Concrete**	
Tensile strength (MPa)	1.9	2.6
Tensile stress point I (MPa)	1.9	2.6
Strain at point I (%)	0.000072	0.000082
Tensile stress point J (MPa)	1.9	2.6
Tensile strain point J (%)	0.0016	0.0021
Tensile stress point k (MPa)	10	10
Tensile strain point K (%)	0.015	0.015
Ultimate strain (%)	0.015	0.015
Crack band width	Rotating	
Compressive behavior	**Fib model code for concrete structure 2010**	
Compressive strength (MPa)	18.9	18.9
Strain at maximum stress (%)	0.021	0.021
Strain at ultimate stress (%)	0.035	0.035

infill wall and the RC frame. It is important to mention that most of the required parameters to define the selected material models in DIANA FEA are taken from the experimental case-study selected for calibration purposes (Section 2), while other parameters were taken from the literature, and at the same time by fitting the numerical results to the experimental ones (especially the parameters for the masonry infill wall model and for the interface model). The required parameters of the Coulomb Friction model are presented in Table 4.

TABLE 4 Parameters of the Coulomb friction interface model

Coulomb friction interface model	Y-direction (column-infill interface)	X-direction (beam-infill interface)
Normal stiffness (Kn)	6 kN /mm^3	3 kN /mm^3
Shear stiffness (Ks)	0.06 kN /mm^3	0.03 kN /mm^3
Cohesion (C)	1 N/mm^2	1 N/mm^2
Friction angle (φ)	30 degree	30 degree
Dilatancy (ψ)	0	0
Tensile strength	1^{-10}N /mm^2	1^{-10}N /mm^2

The masonry-infilled RC frame models with and without TRM are loaded with a constant axial load on the top of each column (to represent the axial load imposed at each story in the test specimens), and they are subjected to the cyclic lateral displacement loading, similar to that of the experimental specimens (Figure 2). The weight of the concrete members which were not modeled due to the 2D simplification followed in this study, are also considered as a dead load (axial loads) equal to 0.9 kN along the length at the top of each column in the numerical models as shown in Figure 2. The loading scheme of the experimental specimen is simulated by applying displacement loading at the three stories of the numerical models (five and seven cycles of displacement loading for the unretrofitted and retrofitted infilled frame, respectively). Point prescribed deformation equal to 1 mm is applied at each of the nodes at the end of each floor as shown in Figure 2, and then different factored load combinations are created for the unretrofitted and retrofitted model to represent the non-uniform height-wise distribution of the displacement. The evolution of the displacement loading is done through the analysis procedure, and it is discretized in loading steps using an automatic incrementation method in which both the number of steps and the corresponding size of each step are automatically computed by DIANA FEA. The criterion used to stop the iteration process is defined in terms of energy with a tolerance value ranging from 10^{-4} to 10^{-6}.

The numerical models are validated by comparing the results obtained from the non-linear displacement-controlled cyclic analysis of the infilled frame model with and without TRM with the corresponding ones obtained from the experimental study conducted by Koutas et al.[49] The base-shear versus the top-floor displacement curves (hysteresis curves) as obtained from the experiment (blue line) and from the numerical analysis (red line) for the infilled frame without and with TRM is given in Figure 3A and B, respectively. From Figure 3A and B it is observed that the difference between experimental and numerical results is relatively small, except for the last cycles of loading where this difference is more pronounced equal to 20%. The peak base-shear of the infilled frame model is underestimated by about 4–13% during the positive direction of loading, while during the negative one it is overestimated by about 6–23% in comparison with the corresponding ones obtained from the experiment. For the retrofitted infilled frame, the peak base-shear in each cycle of loading is either overestimated or underestimated, by a percentage of less than 10%, except at the last cycle of unloading where the numerical model overestimates the peak base-shear of the retrofitted infilled frame by 18%. Figure 3C, D, E, and F show the experimental (blue line) and numerical results (red line) in terms of global stiffness and dissipated energy of the unretrofitted and retrofitted infilled frame in relation to the number of cycles of loading. From Figure 3C and D it is observed that the global stiffness of the unretrofitted and of the retrofitted infilled frame model is either overestimated or underestimated by a percentage smaller than 12 % compared to that obtained from the experiment. From Figure 3E and F it is observed that the dissipated energy of both infilled frame models is overestimated by about 8–12% compared to the real one during the first cycles of loading (first to fourth). For the rest cycles of loading (last two), the dissipated energy is overestimated by about 15–22%. The discrepancy between the experimental and numerical results may depend on the analysis convergence and on the nonlinearities that were introduced in the last cycle of loading during the experiment (brittle failures due to soft-story mechanism at the first floor). Besides that, both models are capable of simulating the in-plane behavior of the unretrofitted and retrofitted masonry-infilled RC frame under cyclic loading with good accuracy in terms of base-shear, shear capacity, global stiffness, and dissipated energy.

Figure 4 shows the crack propagation in the unretrofitted and retrofitted infilled frame at the first and second floor, respectively, as observed in the test specimen and in the numerical model during the fifth and fourth cycle of loading.

From Figure 4 it is observed that the crack pattern that occurred at the first floor on the infilled fame during the fifth cycle of loading is accurately reproduced by the numerical model where horizontal sliding cracks and stair-step-type cracks are developed at the diagonal and at the loaded corners of the infill wall, while shear cracks are developed at the top of both columns in the area which contacted the diagonal of the infill wall (indicating the shear failure of the columns).

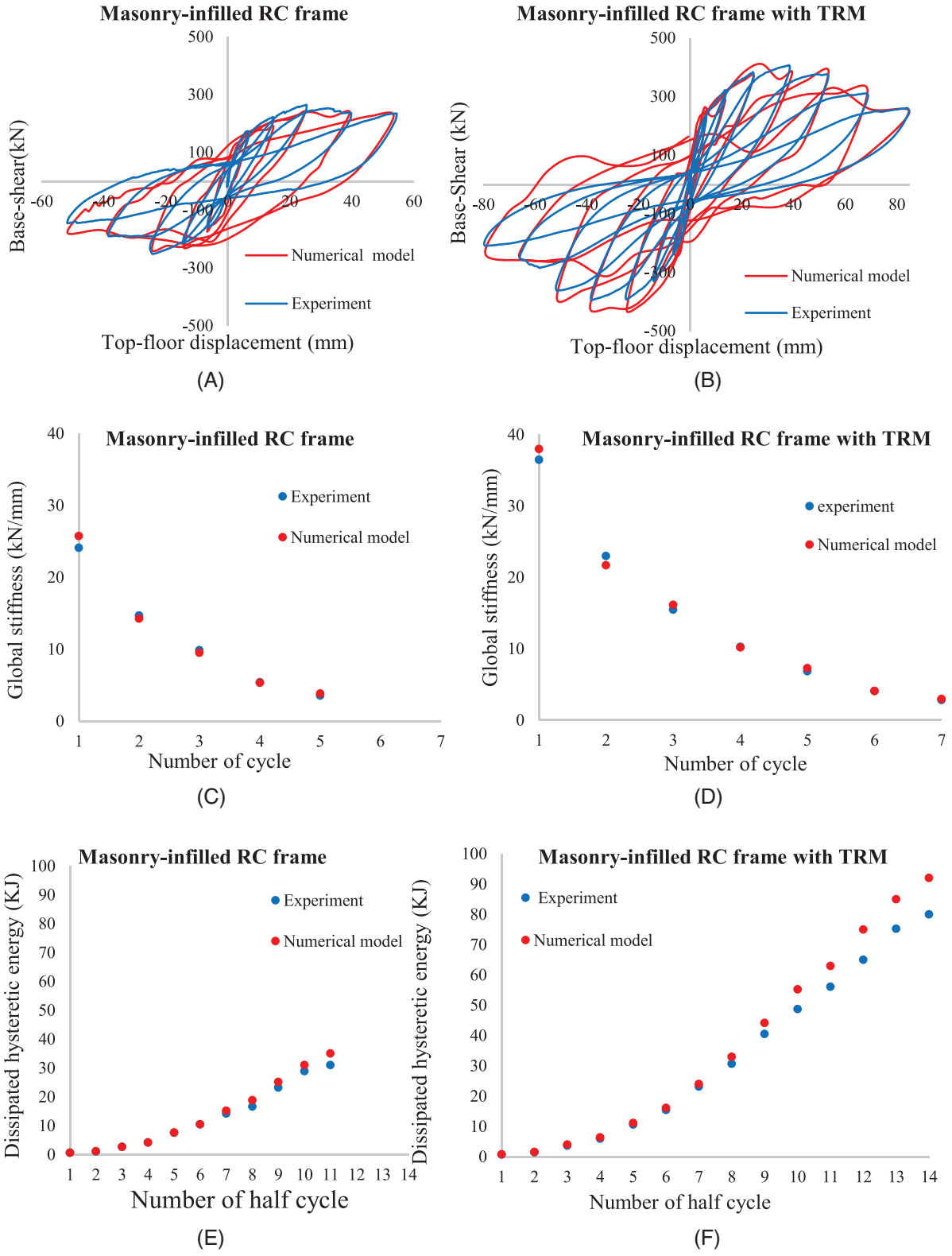

FIGURE 3 Comparison of the experimental and numerical results in terms of base-shear versus top-floor displacement for the (A) unretrofitted infilled frame, and (B) for the retrofitted infilled frame, in term of global stiffness for the (C) unretrofitted infilled frame, and (D) for the retrofitted infilled frame, and in terms of dissipated energy for the (E) unretrofitted infilled frame, and (F) for the retrofitted infilled frame,

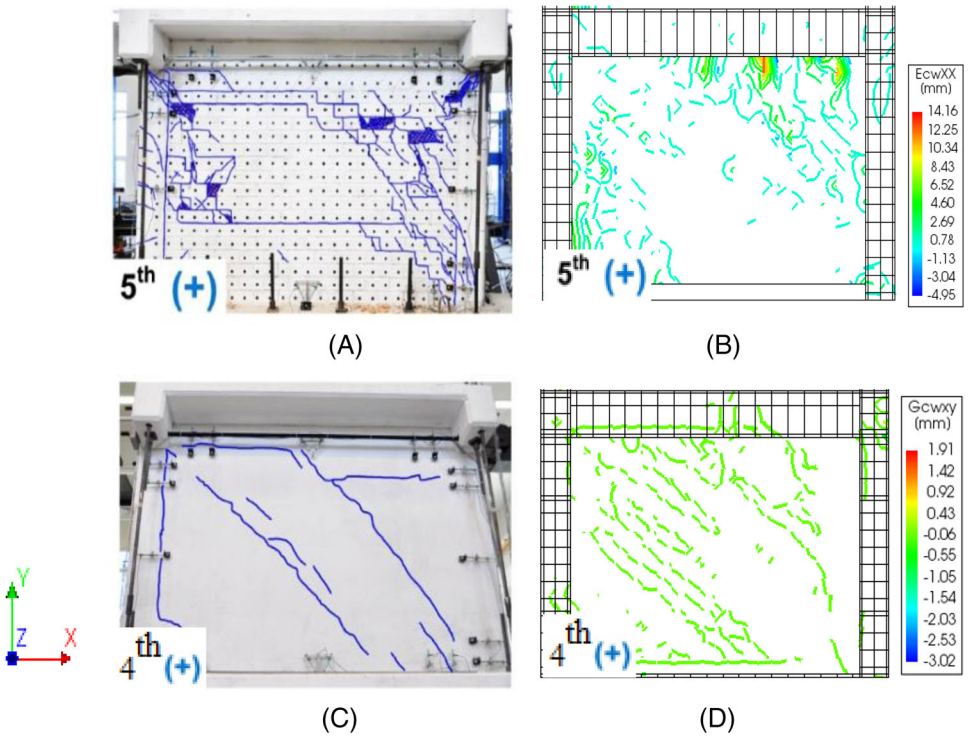

FIGURE 4 Crack propagation at infilled frame during the fifth cycle of loading at the first floor as it occurred in (A) the experiment[49] and (B) in the numerical model,[51,68] and crack propagation in the retrofitted infilled frame during the fourth cycle of loading at the second floor as it occurred in (C) the experiment[49] and (D) in the numerical model.[51,68]

Comparing Figure 4C with Figure 4D, it is observed that the crack pattern developed on the second floor in the retrofitted infilled frame is accurately reproduced by the numerical model since the shear cracks, which are formed on the TRM at the diagonal of the infill wall and close to the loaded corner of the infill wall, are in the same location as in the experimental specimen. More details regarding the validation of the unretrofitted and TRM-retrofitted three-story masonry-infilled RC frame model at the local level can be found in Filippou.[67]

Therefore, the results obtained from the non-linear cyclic analysis on the unretrofitted, and the retrofitted three-story masonry-infilled RC frame are compared to those obtained from the experimental case-study, and they show acceptable degree of accuracy at the global and local level. Hence, these numerical models can be used to perform parametric studies, as it will be presented in the next section.

4 | PARAMETRIC STUDY

The validated three-story masonry-infilled RC frame model with and without TRM, as presented in the previous section, is used to perform a parametric study to investigate the influence of different size of central openings on the lateral response of masonry-infilled RC frames (Section 4.1), and then to assess the effectiveness of using the TRM for the seismic retrofitting of masonry-infilled RC frames with openings (Section 4.2). In order to further validate the numerical models and enhance the reliability of this parametric study, the influence of different size of central openings on the lateral response of infilled frames as obtained from the current study is compared with that obtained from relevant past studies. To achieve a reasonable comparison, the location, the size, and the geometry of the openings were selected in such a way to match those used in earlier studies. Specifically, it was selected to have an opening that ranges from 5% to 27%, as given in Table 5 (square and rectangular shape), in the central part of the infill wall upon its diagonal and slightly closer to the top side of the infilled frame (Figure 5).

The notation of the model specimens is O (%) or SO (%) where the O denotes the unstrengthened infilled frame with Opening, and SO denotes the TRM-Strengthened infilled frame with Opening, and the percentage denotes the ratio of the opening area to the infill wall area. Three reference cases were considered in this study as follows: the masonry-infilled

TABLE 5 Geometric characteristics of the masonry-infilled RC frame model with openings, with and without TRM

Model name without TRM	Model name with TRM	Length of opening (L) (mm)	Height of opening (H) (mm)	Length of infill (mm)	Height of infill (mm)	Percentage ratio of opening area to infill area (%)
O (0%)	SO (0%)	0	0	2270	1670	0
O (5%)	SO (5%)	454	445	2270	1670	5
O (8%)	SO (8%)	681	445	2270	1670	8
O (12%)	SO (12%)	681	668	2270	1670	12
O (16%)	SO (16%)	908	668	2270	1670	16
O (20%)	SO (20%)	1135	668	2270	1670	20
O (27%)	SO (27%)	1362	780	2270	1670	27
O (100%)	SO (100%)	2270	1670	2270	1670	100

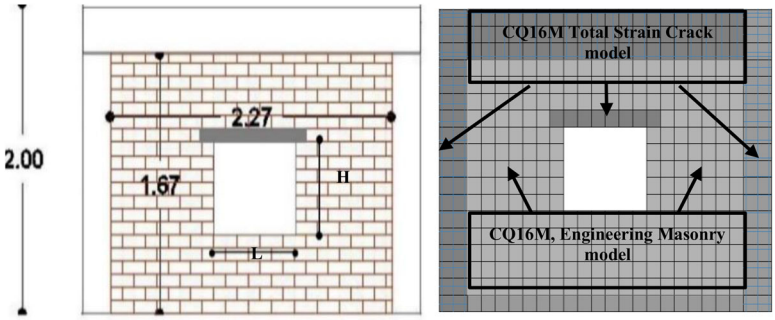

FIGURE 5 (A) Geometry of the masonry infill wall with central opening, and (B) details of FE masonry-infilled RC frame model with central opening

RC frame without openings, O (0%), the masonry-infilled RC frame without openings with TRM, SO (0%) and the bare RC frame, O (100%). It is important to mention that the numerical models of this study were developed following the same modeling scheme with the validated numerical model as presented in the previous section, while the convergence criterion of the non-linear cyclic analysis is modified when it is needed. Adding to this, in the numerical models of the infilled frames with openings, a lintel-beam in the upper part of the central window opening is considered, as shown in the Figure 5B, which is modeled by plane-stress elements while the concrete material model is adopted for these elements.

4.1 | Effect of different size of central openings on the in-plane behavior of the three-story masonry-infilled RC frames subjected to cyclic loading

In this part of the paper, the influence of different sizes of centrally located window openings, varying from 5% to 27%, on the lateral response of the three-story masonry-infilled RC frame subjected to cyclic loading is investigated. This is achieved by performing a parametric study through a non-linear cyclic analysis on the validated three-story masonry-infilled RC frame model considering different size of central openings (Table 5). The numerical models were developed following the same modelling scheme as for the validated numerical model of the three-story masonry-infilled RC frame without openings (Section 3), and they are subjected to five cycles of prescribed displacement loading.

The results obtained from the non-linear cyclic analyses are given in Figure 6 in terms of envelope curves derived from the base-shear versus top-floor displacement diagrams (hysteresis curves, positive direction of loading), which will be presented in the next section.

From Figure 6, it is observed that the presence of a central opening influences the lateral capacity of the three-story masonry-infilled RC frame under in-plane cyclic loading, since as the area of the central opening increases from 8% to 27% the base-shear and the stiffness (slope of envelope curves in Figure 6) of the infilled frame both decrease by 10% to 60%. Considering the infilled frame with 12% and 27% opening at the stage of maximum base-shear, which corresponds to lateral top-floor displacement equal to 35 and 38 mm (top-story drift ratio equal to 0.63%), respectively, it is observed that

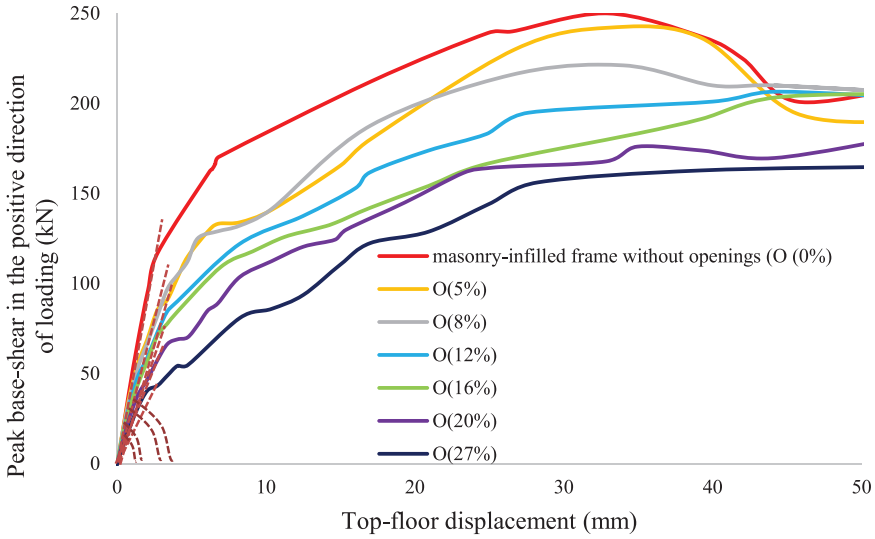

FIGURE 6 Envelope curves obtained from the base-shear versus top-floor displacement curves in the positive direction of loading for the masonry-infilled RC frame model with central opening varying from 5% to 27%

their maximum base-shear decreases by about 15% and 31%, respectively, compared to that of the infilled frame without opening. The latter observations are almost the same with those reported by Kakaletsis and Karayannis,[27] where they found experimentally that the maximum base-shear of the infilled frame with opening equal to 12.5% and 25% decreases by 19% and 32%, respectively, compared to the infilled frame without openings, which leads to the validation of the model.

The numerical models of infilled frames with openings developed in this study are further validated using past experimental studies conducted by Kakaletsis and Karayannis,[25,27] and Tekeli and Aydin,[72] and numerical studies conducted by Akhoundi et al.[73] and Ahani et al.[74] Depending on the available data of each of the above studies, it is decided to use either the envelope curve obtained from the base-shear versus displacement diagram (hysteresis curve) or from the push-over curve. The comparison of the results of the above-mentioned studies with the ones of the current study is given in Figure 7 in terms of the base-shear-ratio, which is the ratio of the base-shear of the infilled frames with openings divided by the base-shear of the infilled frame without openings (solid infilled frame). This ratio, since it is less than one, indicates the decrease in the base-shear of the infilled frames caused by the presence of a central opening. According to the current study, the base-shear of the infilled frame with 8% central opening is about 0.7–0.8 times that of the base-shear of the solid infilled frame, which corresponds to a decrease of the base-shear equal to 20%-30%, at a corresponding lateral displacement ranging from 0.5 to 20 mm (Figure 7A). This decrease is almost the same with that resulted from the study conducted by Tekeli and Aydin[72] and Ahani et al.[74] as shown in Figure 7A (comparing the dashed-blue and the dashed-green curve with the solid-red curve). From Figure 7D it is observed that, according to the current study the base-shear of an infilled frame with central opening equal to 20% is about 0.5–0.7 times that of the solid infilled frame after the 0.5 mm lateral displacement, which is almost the same ratio with that resulted from the study conducted by Ahani et al.[74] (comparing the dashed-green curve with the solid-red curve). From Figure 7, it is also observed that the discrepancy between the results obtained from the current study with those obtained from the selected studies is more pronounced as the lateral displacement increases, with an average difference ranging from 10% to 30%. This difference is the same with that obtained by comparing the base-shear ratio of the Akhoundi et al.[73] study with that of Ahani et al.[74] study as shown in Figure 7A, D, and E (comparing the dashed-green curve with the dashed-purple curve). The discrepancy between the results obtained from the experimental or numerical studies conducted aiming to examine the influence of openings on the lateral response of masonry-infilled RC frames (including the current study) may depend on a large number of different parameters involved in this type of structure in each case, which may affect the results, such as (1) the geometry and mechanical properties of the infill wall, (2) the geometry and mechanical properties of the surrounding frame, (3) the characteristics of the infill–frame interface, (4) the scale of the tested specimens, (5) the load application scheme, (6) the boundary conditions, (7) the accuracy of the nonlinear analysis, and (7) the quality of the materials used and the workmanship. Considering all the above, it can be concluded that the three-story masonry-infilled RC frame model with central openings ranging from 5% to 27% used in this parametric study can predict the real response of such type of structure subjected to in-plane cyclic loading with good accuracy.

The influence of the central opening ranging from 5% to 27% on the lateral capacity of masonry-infilled RC frame is given in Figure 8 in terms of global stiffness versus the number of cycles of loading, and in terms of dissipated energy in relation to the number of half cycles of loading.

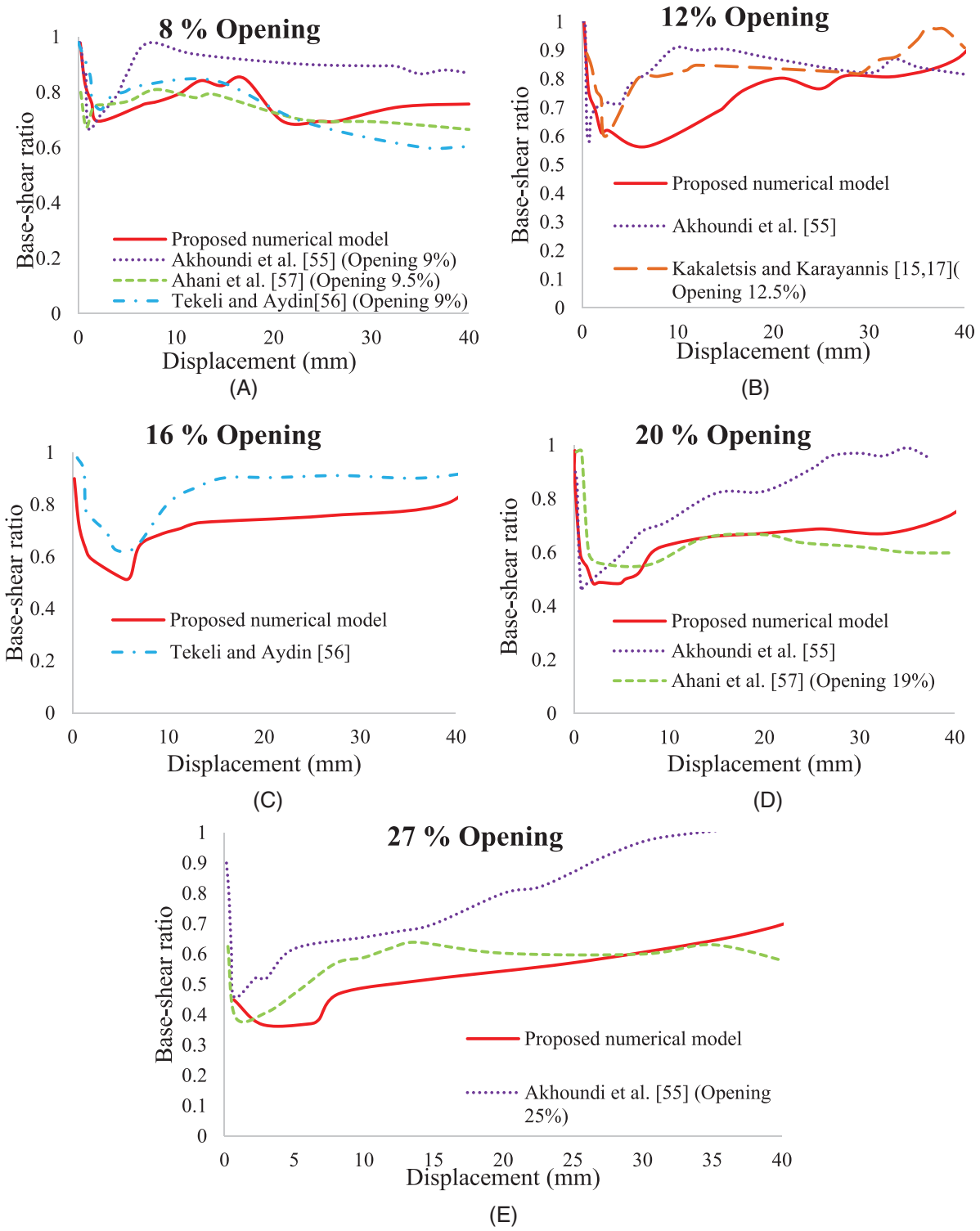

FIGURE 7 The decrease in the base-shear of infilled frame caused by the presence of (A) 8%, (B) 12%, (C) 16%, (D) 20%, and (E) 27% central opening as obtained from the studies conducted in the past and from the current study

From Figure 8, it is observed that the presence of the central opening influences the global stiffness and the dissipated energy of the three-story masonry-infilled RC frame under in-plane cyclic loading, since as the area of the central opening increases from 8% to 27% the global stiffness and the dissipated energy of the infilled frame both decrease by about 5% to 60%. Specifically, from Figure 8, it is observed that the global stiffness and dissipated energy of the infilled frame with central opening ranging from 5% to 8% both decrease by about 5–18% compared to the corresponding ones of the infilled

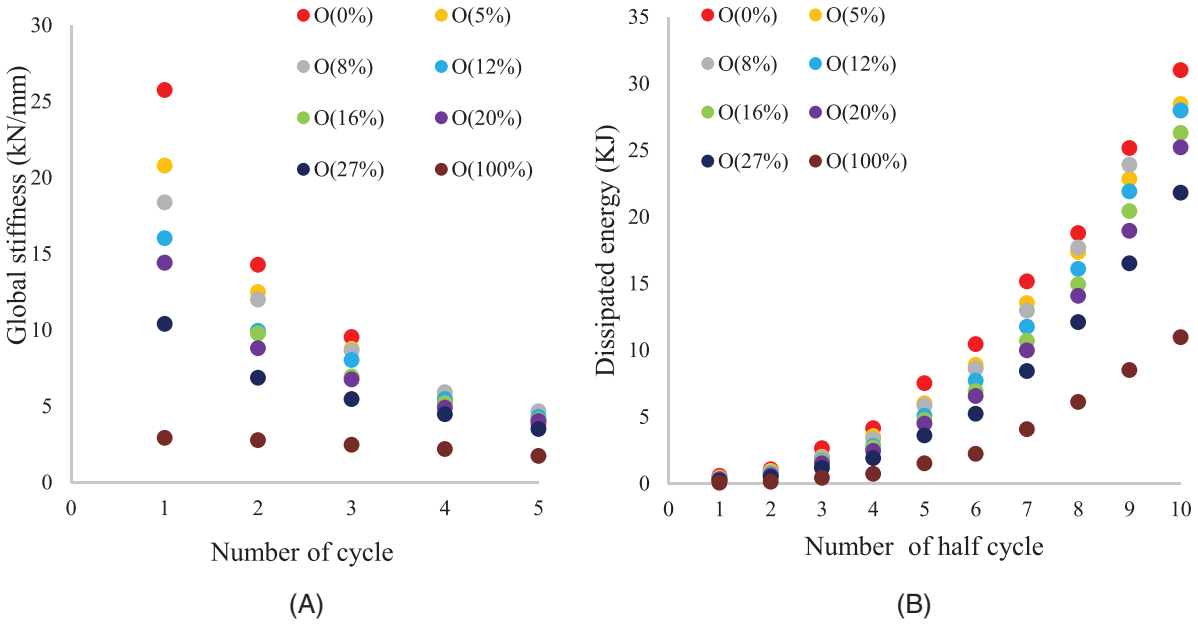

FIGURE 8 Effect of central openings on the lateral capacity of the masonry-infilled RC frame subjected to cyclic loading in terms of (A) global stiffness and (B) dissipated energy

frame without opening for all cycles of loading, except of the stiffness and of the dissipated energy at the first cycle of loading, where both decrease by about 13%-28%. It is also observed that the dissipated energy of the infilled frame with opening equal to 27%, during the first cycle of loading, decreases by about 57% compared to that of the infilled frame without openings, which is almost the same decrease reported in Kakaletsis and Karayannis[27] study (for a 25% opening, the dissipated energy decreases by 50%). In the same study, the authors found that the dissipated energy of the infilled frame with 12.5% opening decreases by 20% compared to that of the infilled frame without openings, which is the same decrease observed in this study as shown in Figure 8. Similar results regarding the global stiffness and dissipated energy of infilled frames with central openings subjected to lateral loading are obtained from the experimental and numerical studies carried out by Mallick and Garg,[24] Liauw,[75] Fiorato,[76] Mosalam et al.[77] Kakaletsis and Karayannis,[27] and by Morandi et al.[78] Finally, according to the current study, the global stiffness, and the dissipated energy of the infilled frame with 100% opening (bare frame) are both decreased by about 50%-86% compared to the corresponding ones of the infilled frame with any central opening percentage. The latter observation is also supported by Asteris et al.[22,62,79] and Kakaletsis and Karayannis.[25] The above-mentioned observation leads to the validation of the three-story masonry-infilled RC frame model with central openings developed in the current study.

From the previous observations, it can also be concluded that the stiffness of the masonry-infilled RC frame decreases with the increase of the opening area, but this decrease is more pronounced during early lateral loading. The trend of the variation of the initial stiffness of the infilled frame due to the presence of an opening, as obtained from the present study, is given in Figure 9A and it is compared to the numerically obtained one by Syrmakezis and Asteris,[1] Asteris et al.,[2,8] Surendran,[80] Cetisli,[81] and by Akhoundi et al.[73] From this figure, it is observed that the variation of the initial stiffness as obtained from the current study is almost similar to that obtained from relevant past studies. The results of the present study are used to perform multiple regression analysis in order to obtain the best-fit data. Based on this fitting, the following relationship for the reduction factor of the stiffness of the infill wall due to the presence of central openings is proposed:

$$\lambda_{\text{opening}} = 1 - 2.16a_w^{0.32} + a_w^{0.16} \quad (1)$$

where a_w is the percentage of the opening area expressed as a decimal number.

The proposed stiffness reduction factor (Equation 1) is also compared with the relevant ones provided by Cetisli[81] and Asteris et al.[8] as shown in Figure 9B. The proposed equation is almost similar to the corresponding one obtained from the Cetisli[81] study, where the stiffness reduction factor is calculated as $\lambda = 1 - 2a^{0.5K_1K_2} + a^{K_1K_2}$, where a is the ratio of area of the opening to the area of the full infill wall, K_2 is a factor representing the effect of the opening location (if the opening is centered this value is equal to 1 according to Cetisli[81]), and $K_1$is a factor representing the effect of the wall

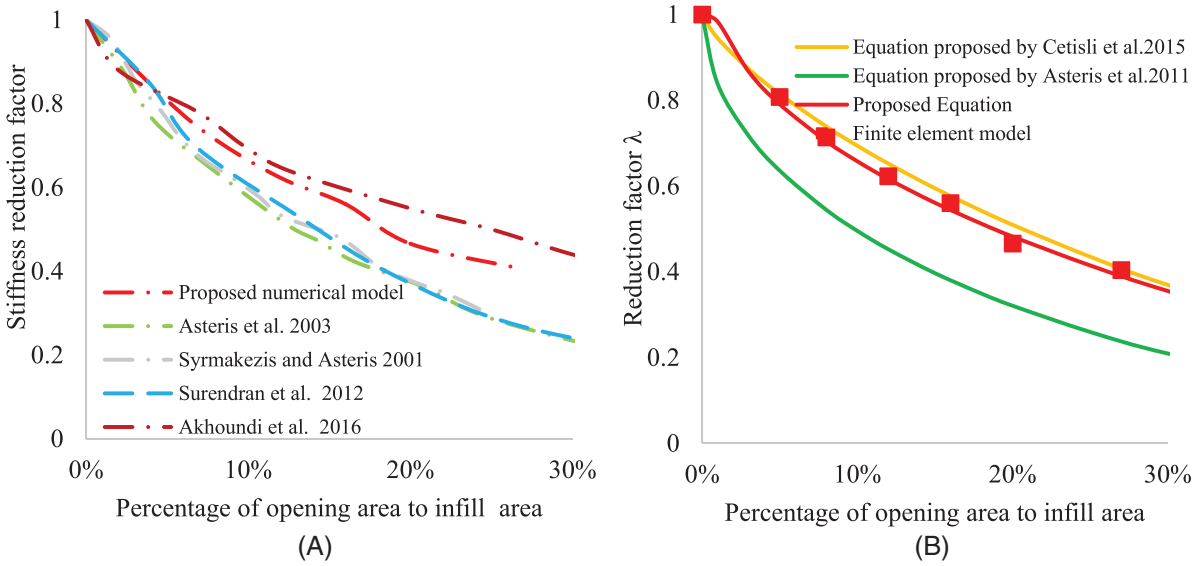

FIGURE 9 Stiffness reduction factor in relation to the opening area percentage as obtained from (A) the numerical model, and from (B) the proposed equation (Eq.1) in comparison with the corresponding ones of previous studies

TABLE 6 Initial stiffness of the infilled frame with different central opening percentage as obtained from simplified macro-model, and as obtained from the numerical analysis

Opening percentage	0%	5%	8%	12%	16%	20%	27%
$K_{elastic}$ (Mainstone 1974)	36.25	29.29	25.87	22.58	20.318	16.88	14.66
$K_{elastic}$ numerical model	34.52	26.88	25.77	22.05	20.76	19.12	15.3

dimensions (Length/height) and it is calculated as follows $K_1 = 1+0.4$ (L/H) (this value is equal to 1.54 since the length of the infill wall is equal to 2270 mm and the height is equal to 1670 mm as shown in Table 5). Thus, according to Cetisli[81] if the opening is centered, and the length to height ratio of the infill wall is equal to 1.35, the stiffness reduction factor is calculated as follows $\lambda = 1 - 2a^{0.77} + a^{1.54}$ which leads to the same results as obtained from proposed stiffness reduction factor ((Equation 1).

The proposed reduction factor can be used with an equivalent strut model, for simulating masonry-infilled frames with openings where the equivalent strut model is a macro-model for everyday practice.[82–85] Following this, Table 6 presents the initial stiffness of the infilled frame with central opening ranging from 5% to 27%, which is obtained by using the proposed stiffness reduction factor (Equation 1) with the empirical equation proposed by Mainstone,[83] which is a widely used approach (recommended by FEMA 306 guidelines[86]). Also, Table 6 shows the initial stiffness of the infilled frame with central opening ranging from 5% to 27% as obtained from the current numerical model (the initial slope of the curves in Figure 6). Based on Table 6, it is observed that the results obtained following a macro-model approach (using the Mainstone's[83] empirical equation and the proposed stiffness reduction factor ((Equation 1)) are in agreement with those obtained in this study through the micro-modeling approach. Hence, the proposed stiffness reduction factor (Equation 1) can be used to modify the equivalent strut stiffness of infilled frames in case of the presence of openings. It is important to note that the proposed reduction factor is applicable for infilled frames with central openings along the diagonal since the effect of the location of the openings on the lateral response of infilled frames is not considered in this study. In addition, extreme cases where the openings are extended to full height or full width of the infilled frame cannot be covered by the proposed equation. Further studies are needed to extend this to other cases.

Figure 10 shows the shear stress distribution and the deformed shape of the three-story masonry-infilled RC frame with central opening ranging from 5% to 27%, during the fourth cycle of loading (maximum base-shear) in the positive direction of loading.

Figure 10 shows that high shear stresses are concentrated in the first floor, somewhat less in the second floor and almost no shear stresses in the third floor. It also shows that the deformation along the height of the structure is not linearly distributed especially in the case of large openings, since the inter-story deformation along the height of the second and

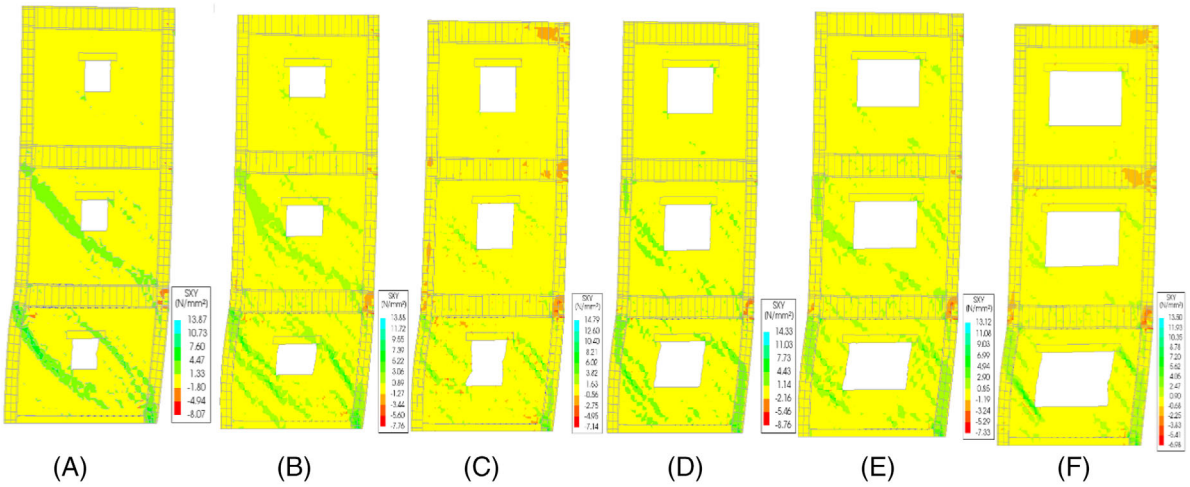

FIGURE 10 Shear stress distribution in the masonry-infilled RC frame with central opening equal to (A) 5%, (B) 8%, (C) 12%, (D) 16%, (E) 20%, and (F) 27%, during the fourth cycle of loading in the positive direction

third floor of structure is almost the same and completely different from that of the first floor (Figure 10D, E, and F), which indicates the formation of a soft-story mechanism at the first floor. From Figure 10, it is also observed that high shear stresses are concentrated at the corners of the opening, and they propagate towards the loaded corners of the infill wall where the diagonal compression path is developed. Adding to this, high concentration of shear stresses is observed at the beam-column joints, and at the ends of the columns in the area that they are in contact with the diagonal of the infill wall at the first floor. This occurs mainly at the first floor in all three-story masonry-infilled RC frames with any opening percentage. It is further observed that as the central opening area increases the shear stresses are increased and they are more spread over the surface of the infill wall, since they are transmitted from the upper and lower parts of the opening to the sides of it, and they then propagate to the bounding frame, as shown in Figure 10 C, D, E, F. Thus, according to the current study the following combination of failure modes in the infilled frame with openings occur due to the interaction of the infill wall with the RC frame: corner crushing, diagonal cracking, and sliding shear. Eventually, the frame failure mode occurs, which consists of the failure of beam-column joints, and of the shear failure of the columns at the first floor of the structure. The frame failure mode is associated with a weak frame and with weak joints in the frame (non-seismic design and detailing of RC frame), leading to the formation of a short-column mechanism (deformed shape of the column in Figure 10C, D, E, F) after the corner crushing of the infill wall with opening. The same observations to the above were reported in the experimental and numerical studies conducted by Asteris,[2] Kakaletsis and Karayannis,[25] Akhoundi et al.,[73] Tekeli and Aydin,[72] Morandi et al.[78] and by Ahani et al.[74]

Figure 10 clearly indicates that the infill wall with opening acts as multi-diagonal no-tension struts. Specifically, the distribution of the shear stresses over the infilled frame with different percentage of central opening shows that two diagonal struts develop within the infill at the first and second floor passing through the upper-left and lower-right of the infill wall during the positive direction of loading. The increase of the opening area results in the restriction of these struts in a much smaller area of the infill at the top and lower parts of it as it is clearly indicated in Figure 10D, E, F. Based on Figure 10 it can be concluded that the masonry infill wall with openings could be better represented by multi-diagonal no-tension strut elements instead of a single-diagonal strut element. This observation is also supported by several researchers such as Thiruvengadam,[87] Chrysostomou,[88] Crisafulli,[5] Chrysostomou et al.,[9] El-Dakhakhni et.al.,[89–91] and in Crisafulli and Carr.[85] This also reinforces the validity of the proposed numerical model.

4.2 | Effect of the TRM on the in-plane behavior of the three-story masonry-infilled RC frames with central openings subjected to cyclic loading

In this part of the paper, the effectiveness of using the TRM composite material for seismic retrofitting masonry-infilled RC frames with central openings is investigated. This is achieved by performing a parametric study through a non-linear cyclic analysis on the validated three-story masonry-infilled RC frame model with TRM considering different size of central openings, varying from 5% to 27% (Table 5). The numerical models of this study were developed following the

TABLE 7 Comparison of the retrofitted and unretrofitted infilled frame with central opening varying from 5% to 27% and without openings (0%) in terms of peak base-shear in each cycle of loading for the positive direction of loading

		$\frac{V_{max\,i_{retrofitted}} - V_{max\,i_{unretrofitted}}}{V_{max\,i_{unretrofitted}}}$ (%)					
Percentage of opening area to infill area	**0%**	**5%**	**8%**	**12%**	**16%**	**20%**	**27%**
Cycle							
1	53%	76%	80%	98%	90%	90%	88%
2	53%	80%	78%	96%	76%	68%	78%
3	54%	79%	71%	85%	88%	78%	71%
4	60%	64%	64%	94%	97%	78%	69%
5	71%	67%	59%	74%	60%	70%	71%

TABLE 8 Comparison of the retrofitted and unretrofitted infilled frame with central opening varying from 5% to 27% and without openings (0%) in terms of peak base-shear in each cycle of loading for the negative direction of loading

		$\frac{V_{max\,j_{retrofitted}} - V_{max\,j_{unretrofitted}}}{V_{max\,j_{unretrofitted}}}$ (%)					
Percentage of opening area to infill area	**0%**	**5%**	**8%**	**12%**	**16%**	**20%**	**27%**
Cycles							
1	33%	83%	78%	92%	90%	85%	98%
2	42%	50%	51%	89%	84%	84%	95%
3	84%	74%	66%	90%	75%	76%	96%
4	131%	58%	60%	63%	72%	70%	59%
5	114%	57%	46%	60%	55%	28%	30%

same modeling scheme with the validated numerical model of the three-story masonry-infilled RC frame with openings described in Section 4.1 and following the TRM-retrofitting scheme of the numerical model of the TRM-retrofitted three-story masonry-infilled RC frame without openings presented in Section 3. The numerical models of the three-story TRM-retrofitted masonry-infilled RC frame with openings varying from 5% to 27% are subjected to five cycles of prescribed displacement loading.

The results obtained from the non-linear cyclic analysis on the three-story masonry-infilled RC frame model with central opening ranging from 5% to 27% without (dashed-line) and with TRM (solid-line) are presented in Figure 11 in terms of base-shear versus top-floor displacement (hysteresis curves). From Figure 11 it is observed that the TRM contributes to increasing significantly the lateral capacity of the three-story masonry-infilled RC frame with any central opening percentage, since the maximum base-shear, and the area enclosed by the loop in the base-shear versus top-floor displacement diagram in each cycle of loading of the retrofitted infilled frames with openings are almost two times that of the corresponding ones of the unretrofitted infilled frames with openings. This occurs for all infilled frames with any opening percentage. From Figure 11A it is also observed that the retrofitted infilled frame with small opening area equal to 5% behaves similarly to the retrofitted infilled frame without openings (Figure 3B). For the benefit of the reader Tables 7 and 8 show the increase in peak base-shear in each cycle of loading of the retrofitted infilled frame compared to that of the unretrofitted infilled frame with openings varying from 5% to 27%, and without openings (0%), for the positive ($V_{max,i}$), and negative ($V_{max,j}$) direction of loading, respectively.

From Tables 7 and 8, it is observed that the TRM increases the base-shear of the infilled frames with openings ranging from 5% to 27% by about 30% to 98% compared to that of the unretrofitted ones. Furthermore, it is observed that the increase due to TRM in the base-shear of the infilled frames with opening ranging from 8% to 27% for the first three cycles of loading is larger than the one for the retrofitted infilled frame without openings (see the 0% column in the Tables), ranging from 51% to 98% for the former and from 33% to 84% for the latter. Thus, at early stage of lateral loading, the TRM contributes to a significant increase in the lateral capacity of the infilled frames with openings relative to that of the infilled frames without openings. Therefore, from the early lateral loading stage the TRM prevents the large shear deformation of the infill wall, which is due to the presence of the opening, leading to significant increase in the lateral capacity of the

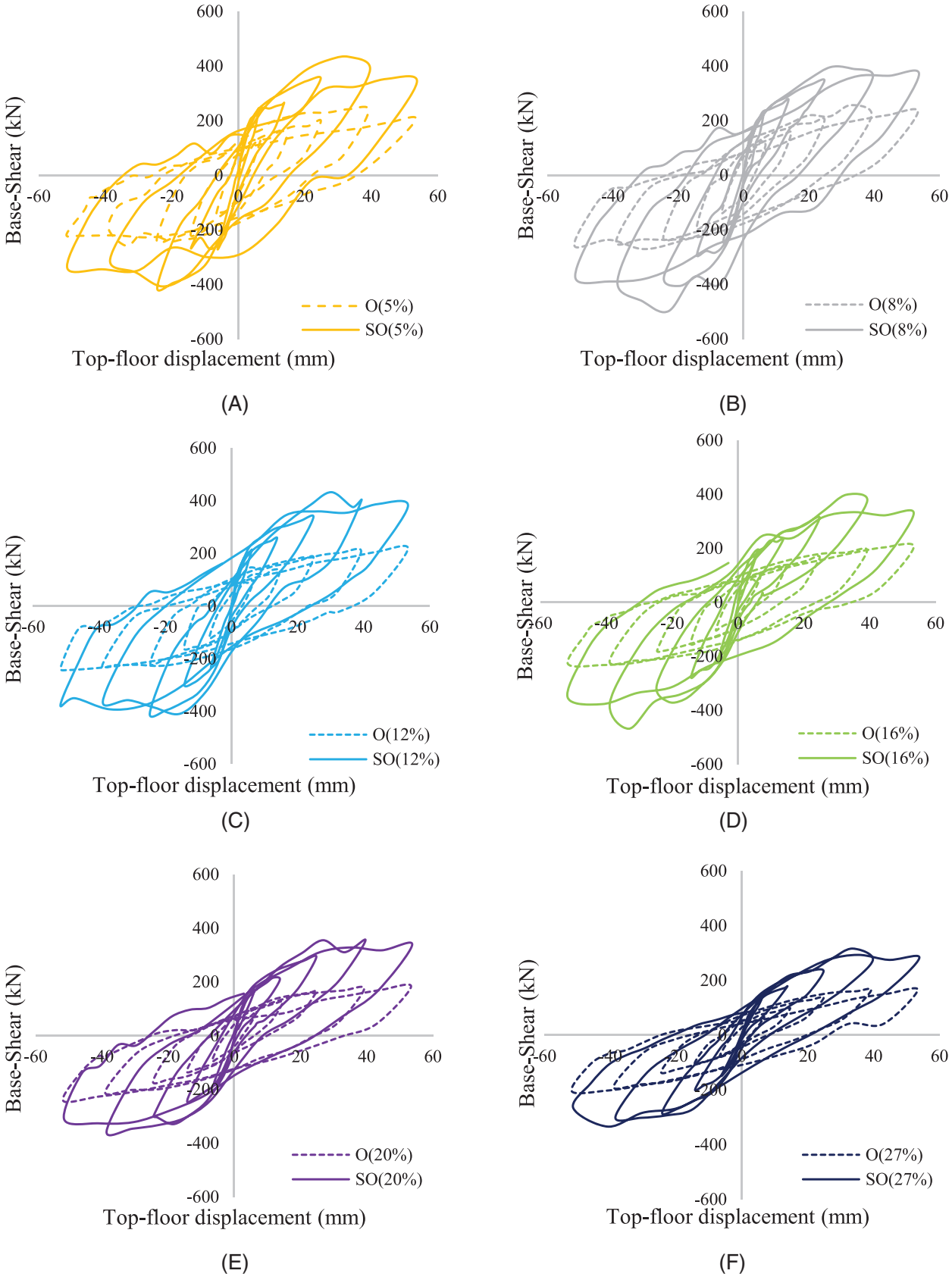

FIGURE 11 Base-shear versus top-floor displacement of the three-story masonry-infilled RC frame with different central opening area percentage without (dashed line) and with TRM (solid line)

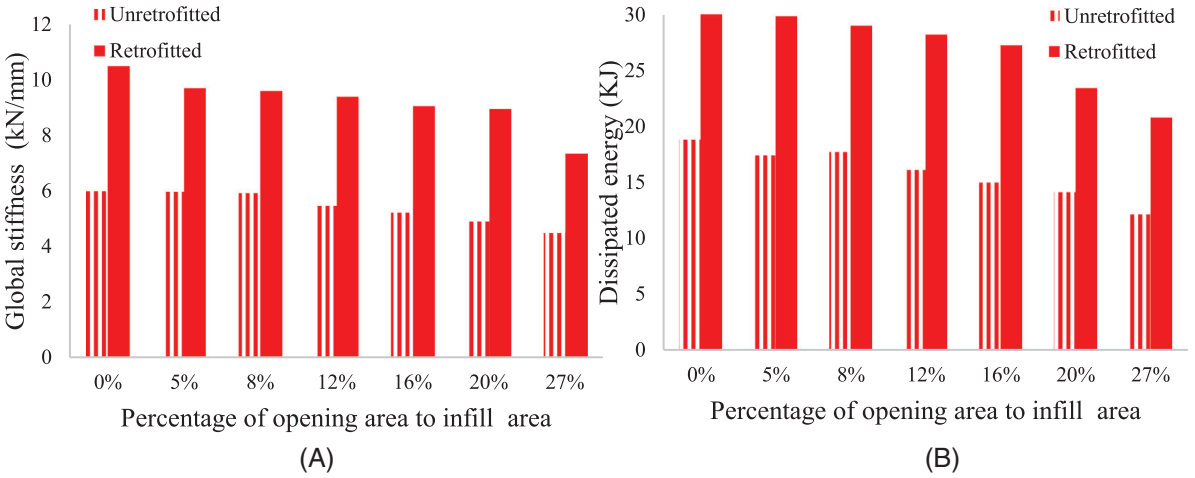

FIGURE 12 Comparison of the retrofitted and unretrofitted infilled frame with central opening varying from 5% to 27% and without openings (0%) in terms of (A) global stiffness and (B) dissipated energy at the fourth cycle of loading

structure. Contrarywise, during the last cycles of loading, it is observed that the increase due to TRM in the base-shear of the infilled frames with opening ranging from 8% to 27%, is smaller than the one for the retrofitted infilled frame without openings (see the 0% column in the Tables), ranging from 28% to 97% for the former and from 60% to 131% for the latter. This is due to the brittle failures that occur in the infilled frame with openings during the last cycles of loading, especially when the opening ranges from 20% to 27% where a short-column mechanism forms (as shown in Figure 10E and F).

Figure 12 presents the global stiffness and the dissipated energy of the retrofitted and unretrofitted infilled frames without openings and with openings varying from 5% to 27% during the fourth cycle of loading, where the maximum base-shear is attained. From Figure 12A, it is observed that the global stiffness of the retrofitted infilled frames with any opening percentage at the maximum base-shear (fourth cycle of loading) is almost two times that of the unretrofitted ones, which leads to an increase equal to 100%. The same increase is observed by comparing the solid infilled frame with and without TRM. Furthermore, from Figure 12B, it is observed that the dissipated energy of the retrofitted infilled frame with any opening percentage during the fourth cycle of loading is about 1.5–1.8 times that of the unretrofitted ones, which leads to an increase equal to 50%-80%. Figure 12 also shows that the global stiffness and the dissipated energy of the retrofitted infilled frame with opening equal to 27% are larger than the corresponding ones of the unretrofitted infilled frame without openings (0%). Thus, the TRM, even in the case of a very large opening, contributes to the increase of the global stiffness and the dissipated energy of the infilled frame with openings, since it provides larger global stiffness and dissipated energy than those of the unretrofitted infilled frame without opening (O%).

The results of the present parametric study are used to perform a regression analysis leading to the following reduction factor of the initial stiffness of the retrofitted infilled frame with central opening:

$$\lambda_{(TRM_opening)} = 1 - 2.0a_w^{0.38} + a_w^{0.15} \quad (2)$$

where a_w is the percentage of the opening area expressed as a decimal number.

The proposed stiffness reduction factor is applicable for TRM-retrofitted masonry-infilled RC frames with central openings along the diagonal of the infill wall (with opening ranging from 5% to 27%). This reduction factor can be used for simulating the TRM-retrofitted masonry-infilled RC frames with openings following the macro-modeling approach where the contribution of externally bonded layers of TRM are considered by introducing an additional term in the equations usually employed for unretrofitted infilled frames. Thus, this proposed reduction factor can be used in the TRM equivalent tie-element model proposed by Koutas et al.[92] and Pohoryles and Bournas[93] in order to predict the lateral strength and stiffness of TRM-retrofitted masonry-infilled RC frames with central openings subjected to lateral loading.

Figure 13 presents the comparison of the proposed stiffness reduction factor for the retrofitted (Equation 2) and for the unretrofitted (Equation 1) infilled frame in relation to the central opening percentage. Comparing the two curves, a sharper decrease in the reduction factor of the unretrofitted infilled frame than the retrofitted one is observed. This is attributed to the full activation of TRM due to the presence of the opening in the infilled frame from an early stage of loading as previously discussed. Furthermore, from Figure 13 it is observed that in the cases where the opening ranging

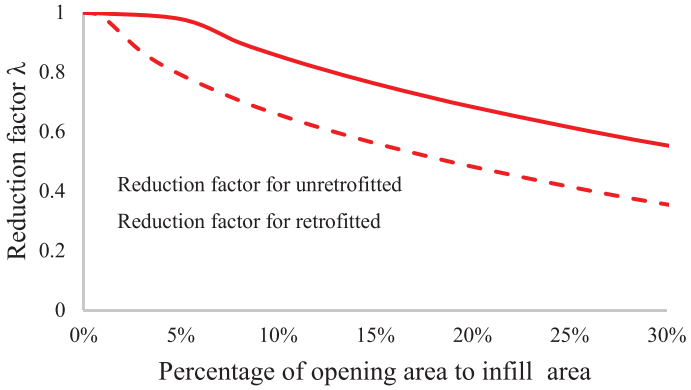

FIGURE 13 Comparison of the proposed initial stiffness reduction factor for the retrofitted and unretrofitted infilled frame with different central opening percentage

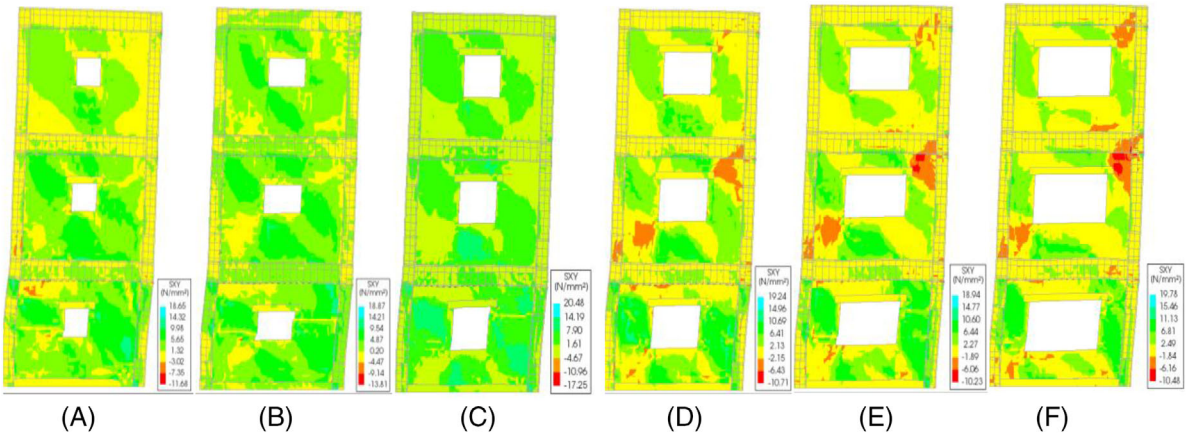

FIGURE 14 Shear stress distribution in the TRM-retrofitted masonry-infilled RC frame with central opening area equal to (A) 5%, (B) 8%, (C) 12%, (D) 16%, (E) 20%, and (F) 27%, during the fourth cycle of loading in the positive direction

from 20% to 30%, the initial stiffness of retrofitted infilled frame is reduced by about 30–60%, while the initial stiffness of unretrofitted infilled frame is reduced by about 50–65%. Therefore, the TRM is able to delay the stiffness degradation of infilled frames due to presence of the opening.

Figure 14 shows the shear stress distribution and the deformed shape of the three-story TRM-retrofitted masonry-infilled RC frame with central opening ranging from 5% to 27%, during the fourth cycle of loading (maximum base-shear) in the positive direction of loading.

From Figure 14, it is observed that the shear stresses are almost evenly distributed in all the three stories of the infilled frame in the case when the opening ranges from 5% to 12% (Figure 14A, B, and C), while as the opening increases from 16% to 27%, high shear stresses are concentrated in the first and second floor, and somewhat less on the third floor (Figure 14D, E, and F). It is also observed that the deformation along the height of the structure is almost linearly distributed in the case when the opening ranges from 5% to 12%, while as the opening increases from 16% to 27% the inter-story deformation signifies the formation of a soft-story mechanism at the first floor (Figure 14D, E, and F). From Figure 14, it is also observed that as the opening area increases, the shear stresses become localized since high shear stresses are concentrated on the TRM at the location corresponding to the corners of the opening, while these shear stresses propagate towards the loaded corners of the infill wall, and to the ends of the columns in the area which is in contact with the diagonal of the infill wall. This occurs mainly at the first and second floor in the three-story TRM-retrofitted masonry-infilled RC frames with opening ranges from 16% to 27% (Figure 14D, E, and F). The high shear stresses on the TRM near the corners of the opening indicates the failure of the infill wall (corner crushing), and the possible rupture and debonding of the TRM at the corners of the opening. Therefore, special attention must be paid for anchoring the TRM along the perimeter of the opening. The anchorage of the textile to the boundaries of the opening is one of the most important details of the TRM-based solution, and it can be performed through different types of elements such as metallic connectors, L-shape GFRP connectors, plastic connectors, textile-based anchors 2), or by extending the TRM retrofitting layer applied to infill walls to the inside boundaries of the opening or by using different length of overlapping of the mesh along the

TABLE 9 Summary of the numerical specimens of three-story masonry-infilled RC frame with TRM by varying the TRM reinforcement ratio in each floor of the structure

Specimen name	First floor	Second floor	Third floor
Reference	Two layers of glass-TRM	One layer of glass-TRM	One layer of glass-TRM
LF1S1	One layer of glass-TRM	One layer of glass-TRM	No strengthening
LF2S1	Two layers of glass-TRM	One layer of glass-TRM	No strengthening
LF3S1	Three layers of glass-TRM	One layer of glass-TRM	No strengthening
DF3S1	Three layers of glass-TRM using 11 mm spacing between the yarns of the textile mesh	One layer of glass-TRM	No strengthening

infill-opening transition. It is important to mention that the possible debonding of TRM from the infilled frame with openings cannot be represented in this study since full bond between an infill wall and the TRM is considered in the numerical models (Section 3).

By examining the shear stress distribution in the unretrofitted and retrofitted infilled frame with central opening ranging from 5% to 27%, it is observed that the TRM contributes to delaying the corner crushing and the diagonal cracking of the infill wall since the shear stresses in retrofitted infilled frames with any opening percentage are more evenly distributed on the infilled frames and they are less localized at the corners of the opening than the ones of the unretrofitted ones (comparing Figure 10 with Figure 14). This indicates that the TRM is effective to avoiding or even preventing brittle failures by transferring the high shear stresses of the infill wall to the TRM as indicated by the multi-stress pattern on the TRM at the first and second floor. Adding to this the maximum shear stresses of the unretrofitted and the retrofitted infilled frame with any opening percentage is equal to $\pm$ 13-20 and $\pm$ 8-14 MPa, respectively. It is also observed that the TRM contributes to delaying or even preventing the brittle failures such as short-column mechanism and the soft-story mechanism in the cases when the opening area ranges from 5% to 27% (comparing Figure 10 with Figure 14). This indicates that the TRM is effective to even preventing the large shear deformation and to delay the brittle failures of the infilled frames due to the presence of large opening.

5 | NUMERICAL SENSITIVITY ANALYSIS

A numerical sensitivity analysis is performed on the validated three-story masonry-infilled RC frame model with TRM, as presented in Section 3, aiming to examine the parameters that can influence the response of masonry-infilled RC frames retrofitted with TRM under cyclic loading such as: the TRM reinforcement ratio and the type of mortar used for binding the textile reinforcement. The same modeling scheme was used for the numerical specimens as for the validated numerical model (Section 3), while the analytical model of TRM proposed by Filippou and Chrysostomou[71] is used in order to facilitate the implementation of the numerical specimens for this parametric study.

5.1 | Effect of the TRM reinforcement ratio on the lateral response of the three-story masonry-infilled RC frame retrofitted with TRM

In this section, the influence of the TRM reinforcement ratio, by means of using different number of TRM layers and different geometry of textile (spacing between the yarns in the textile) on each floor of the TRM-retrofitted three-story masonry-infilled RC frame, on the response of the three-story masonry-infilled RC frame retrofitted with TRM under cyclic loading is investigated through numerical experiments as shown in Table 9.

The notation of the model specimen is (L) or (D) F_ number S_ number, where; the L and D denote the mesh opening (spacing between the yarns) equal to 21 and 11 mm, respectively; the second letter denotes the floor of the three-story infilled frame: F (first floor) and S (second floor); and the number represents the number of TRM layers (1, 2, and 3 TRM-layers). The validated infilled frame model with TRM is considered as a reference case for this study as shown in Table 9. Furthermore, for all the numerical specimens in this parametric study (including the reference case), three layers and two layers of carbon-TRM are used at the ends of the columns at the first and second stories, respectively.

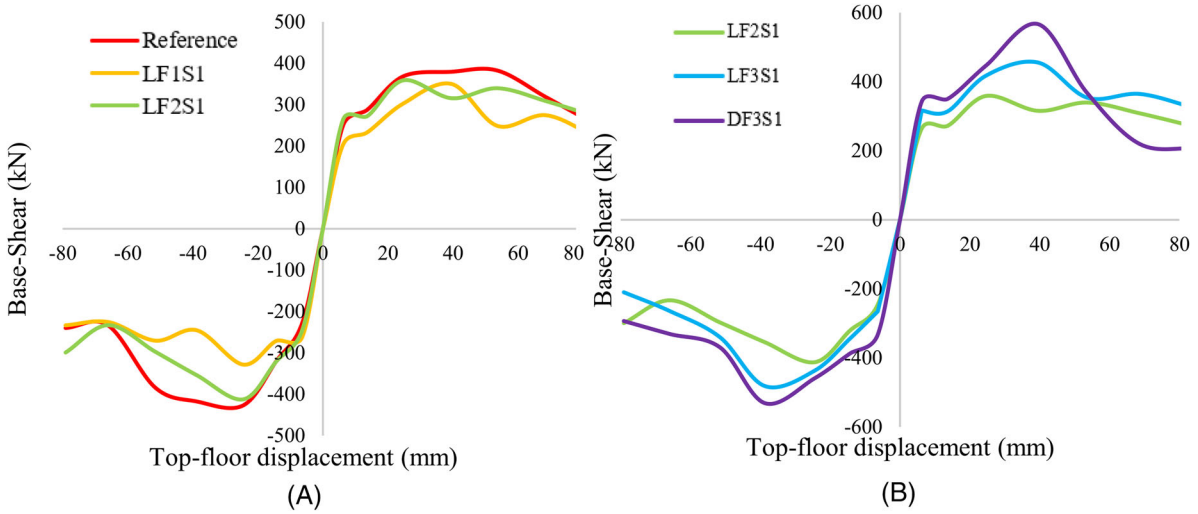

FIGURE 15 Comparison of the results obtained from non-linear cyclic analysis of the (A) the reference specimen (red line), of the LF2S1 specimen (green line), and of LF1S1 specimen (yellow line) and (B) of the LF2S1 specimen (green line), of the LF3S1 specimen (blue line) and of the DF3S1 specimen (purple) in terms of base-shear versus top-floor displacement (envelope curve -peaks)

The results obtained from the non-linear cyclic analysis of the reference specimen (red line), of the LF2S1 specimen (green line), and of LF1S1 specimen (yellow line) are presented in Figure 15A in terms of base-shear versus top-floor displacement (envelope curve -peaks). Figure 15B presents the base-shear versus top-floor displacement (envelope curve -peaks) of the three-story masonry-infilled frame specimen considering one layer of TRM at the second floor, and two and three layers of TRM at the first floor with 21 and 11 mm spacing between the yarns of the textile (LF2S1-green line, LF3S1-blue line and DF3S1-purple).

From Figure 15A, it is observed that there is no significant difference between the reference specimen and LF2S1specimen, while a small decrease (with an average percentage equal to 5%) in the base-shear of the LF2S1 specimen is observed compared to that of the reference specimen. Therefore, the use of TRM at the third floor of the three-story infilled frame retrofitted with two layers of TRM at the first floor and one layer of TRM at the second floor, does not provide any gain to the lateral capacity of the retrofitted structure. Furthermore, from Figure 15A, it is observed that the lateral capacity of LF2S1 specimen is increased by about 30% compared to that of LF1S1 specimen (comparing the green with the yellow line). Therefore, it is important to apply more than one layer of TRM at the first floor in a three-story masonry-infilled RC frame. From Figure 15B, it is observed that the base-shear of the LF3S1 and DF3S1 specimen are significantly increased compared to the corresponding ones of the LF2S1 specimen. Especially, for the LF3S1 and DF3S1 specimen the maximum base-shear is about ± 450 and ± 500 kN, respectively, while for the LF2S1 specimen is about ± 400 kN during the fourth cycle of loading for both directions of loading. Furthermore, this figure shows that the increase on the peak base-shear in each cycle of loading and unloading of the three-story infilled frame retrofitted with one layer of TRM at the second floor, and three-layers of TRM at the first floor (LF3S1 and DF3S1) is increased by 15%-20% compared to the case of using two layers of TRM at the first floor and one layer of TRM at the second floor (LF2S1). This increase is not proportional to that of the TRM reinforcement ratio, since using double amount of TRM reinforcement ratio, for example comparing the LF2S1 specimen with DF3S1 specimen (reinforcement ratio for three layers of TRM with 11 mm mesh opening is equal to 3.2% and for two layers is equal to 1.3%), does not provide double shear capacity of the retrofitted infilled frame.

Figure 16 presents the influence of the TRM reinforcement ratio on the behavior of the three-story masonry-infilled RC frame retrofitted with TRM under cyclic loading in terms of global stiffness, and in terms of dissipated energy.

From Figure 16, it is observed that the global stiffness and the dissipated energy of the specimens with two or three layers of TRM at the first floor and one layer of TRM at the second floor (LF2S1, LF3S2, and DF3S1) are increased by about 10–60% compared to the corresponding ones of the specimen with one layer of TRM at the first floor and second floor (LF1S1) during the first cycles of loading. From Figure 16, it is also observed that the global stiffness and the dissipated energy of the reference specimen, and those of the LF2S1 specimen are almost the same (difference less than 10%-12%), while the global stiffness and the dissipated energy of LF2S1 are increased by about 23% compared to the corresponding ones of the LF1S1 specimen. Thus, the global stiffness and the dissipated energy of the three-story infilled frame retrofitted

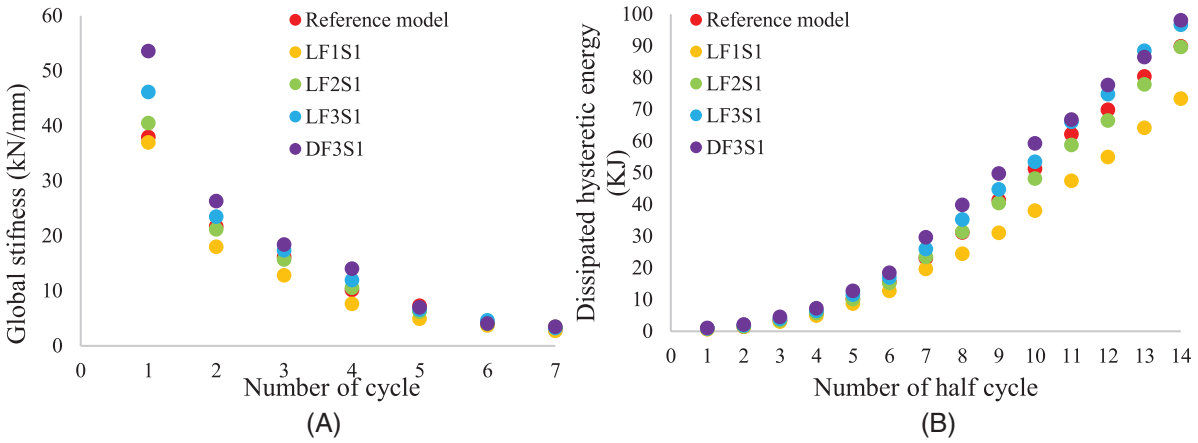

FIGURE 16 Comparison of the results obtained from non-linear cyclic analysis of the masonry-infilled RC frame with different TRM reinforcement ratio in terms of (A) global stiffness and in (B) dissipate energy

TABLE 10 Summary of the numerical specimens of three-story masonry-infilled RC frame with TRM using different types of mortars for binding the textile reinforcement

Name of the model	Name of the mortar used on TRM	Compressive strength (MPa)	Tensile strength (from bending test) (MPa)
Reference (R2C18)	Commercial fiber-reinforced mortar (R2)	18.9	4.3
R2C22	Sika MonoTop-722 Mur (R2)	22	6
R3C33	Sika MonoTop-615 (R3)	33	7
R4C45	Sika MonoTop-627 HP (R4)	45	8
R4C50	TSIRCON PER122 (R4).	50	10

with TRM subjected to cyclic loading are highly dependent on the TRM reinforcement ratio used at the first floor of the structure.

5.2 | Effect of the type of mortar used for TRM on the lateral response of the three-story masonry-infilled RC frame retrofitted with TRM

In this section, the influence of the type of mortar used for binding the textile reinforcement on the effectiveness of using the TRM composite material for retrofitting masonry-infilled frames is investigated. Towards this direction, the validated three-story masonry-infilled RC frame model with TRM is used to perform numerical experiments considering different types of mortars for TRM. For the purpose of this study, four different commercial mortars[94] for the TRM (manufactured by SIKA and TSIRCON company) are selected to be examined as shown in Table 10, where each mortar represents a different class of mortar according to European Standard UNI EN 1504-3[94] (defines four classes of repair mortars as follows: R1 and R2 for non-structural mortar, and R3 and R4 for structural mortar). Table 10 also shows the mechanical properties of each of the mortar examined in this study as given by manufacturer.

The notation of the model specimen is R _ number C _ number, where the letters R and C represent the repair mortar and its compressive strength, respectively, while the first number denotes the class of the mortar (2, 3 and 4) and the second number denotes the value of the compressive strength of mortar. The validated masonry-infilled RC frame model with TRM (Chapter 4) is considered as a reference case for this study as shown in Table 10.

The results obtained from the non-linear cyclic analysis of the reference specimen (R2C18-red line), of the R2C22 specimen (yellow), and of R3C33 specimen (green line) are presented in Figure 17A in terms of base-shear versus top-floor displacement (envelope curve -peaks). Figure 17B presents the base-shear versus top-floor displacement (envelope curve -peaks) of the reference specimen (R2C18-red line), of the R4C45 specimen (blue line), and of R4C50 specimen (purple line).

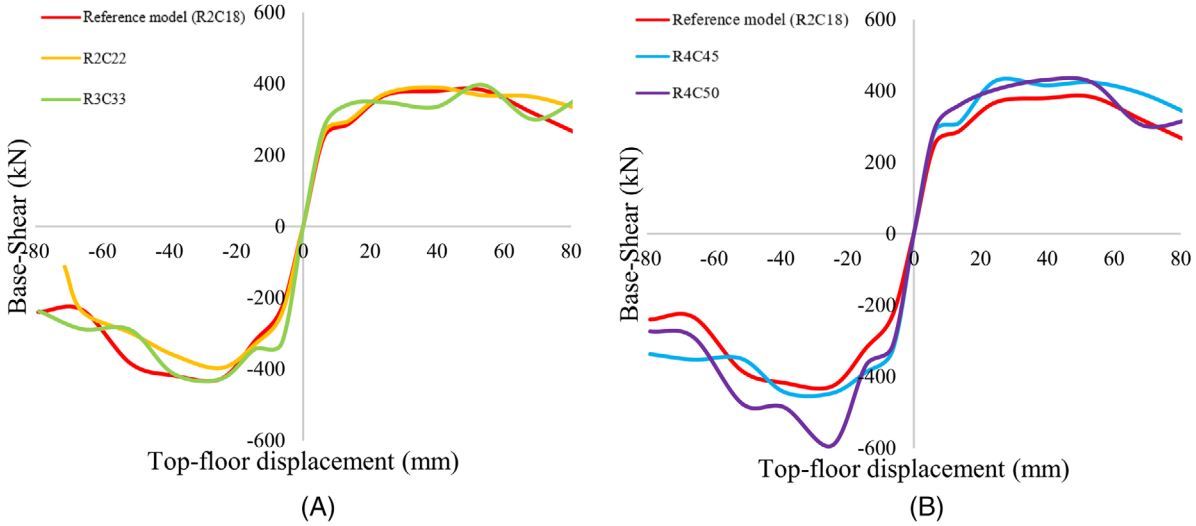

FIGURE 17 Comparison of the results obtained from non-linear cyclic analysis of the (A) reference specimen (R2C18-red line), of the R2C22 specimen (yellow), and of R3C33 specimen (green line) and (B) of the reference specimen (R2C18-red line), of the R4C45 specimen (blue line), and of R4C50 specimen (purple line) in terms of base-shear versus top-floor displacement (envelope curve -peaks)

From Figure 17A, it is observed that the results of the reference specimen and of the R2C22 specimen, where a similar type of mortar is used (R2 class of mortar), are almost the same. Thus, a slight increase in the compressive and tensile strength of the mortar (R2 class of mortar) used for binding the textile reinforcement of 22% and 11% respectively, does not contribute to increase the lateral capacity of the infilled frame retrofitted with TRM. Comparing the results of the reference specimen with those of the R3C33 specimen it is observed that the base-shear of the R3C33 specimen is increased by only about 10%, despite the fact that in the R3C33 specimen almost a double compressive and tensile strength of the mortar is used for the TRM (Table 10). From Figure 17B, it is observed that the peak base-shear of the R4C45 and R4C50 specimen in each cycle of loading is increased by about 10–30% compared to the corresponding ones of the R2C18 specimen (where the compressive and tensile strength of the mortar used in R4C45 and R4C50 specimens is 100–150% and 33–133% higher than the corresponding ones of the mortar used in R2C18 specimen). Thus, the lateral capacity of the infilled frame retrofitted with TRM is not increased proportionally with the increase of the mechanical properties of the mortar used for TRM. This may be attributed to the fact that during the first cycles of loading, where the influence of the compressive strength of the TRM mortar on the lateral capacity of the retrofitted infilled frame is more pronounced compared to its tensile strength, as explained in the next paragraph, the substantial increase of the compressive strength of the mortar does not enhance the compression strut of the infill wall significantly due to the relatively small thickness of the mortar. During the last cycles of loading, where the contribution of the tensile capacity of the TRM to increase the lateral capacity of the retrofitted infilled frame becomes more pronounced than its compressive capacity, as discussed in the next paragraph, the substantial increase of the tensile strength of the mortar does not enhance the lateral capacity of the retrofitted infilled frame significantly due to the fact that at large deformations mainly the textile reinforcement contributes to the lateral capacity of the retrofitted infilled frame (Filippou and Chrysostomou[71]).

Figure 18 shows the comparison of the R4C45 and R4C50 specimen with the reference specimen (R2C18) in terms of global stiffness and dissipated energy. From Figure 18, it is observed that when the compressive strength of mortar is increased substantially by about 150–180% and with an increase in the tensile strength of the mortar, 60–75% (R4C45 and R4C50) relative to the reference specimen (R2C18), the global stiffness and dissipated energy of the infilled frame are increased by about 12–25% during the first cycles of loading and by about 10–15% during the last cycles of loading. This occurs because the influence of the compressive strength of the mortar used for TRM on the lateral capacity of the retrofitted infilled frame is more pronounced compared to the tensile strength of the mortar used for TRM during the first cycles of loading, since the compressive capacity of TRM contributes to enhance the compression strut of the infill wall. Adding to this, as the lateral loading increases, the contribution of the tensile capacity of the TRM to increase the lateral capacity of retrofitted infilled frame becomes more pronounced than the compressive capacity of TRM since at this stage this composite material sustains the high tensile stresses which are transferred from the infill wall to the TRM at local level.

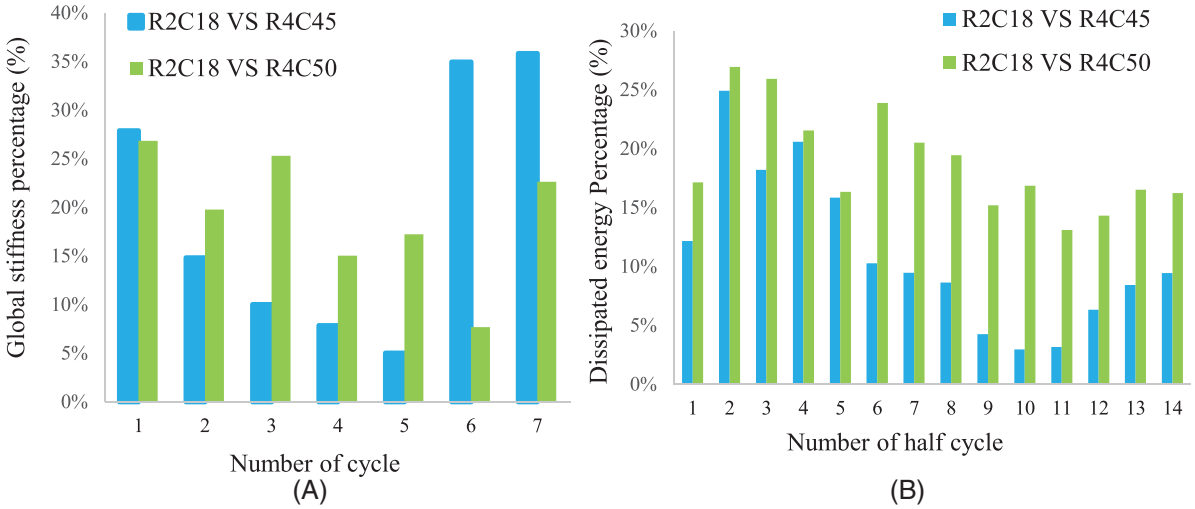

FIGURE 18 Comparison of the R4C45 and R4C50 specimen with the reference (R2C18) in terms of (A) global stiffness and (B) dissipated energy

6 | CONCLUSION

This study aims to assess the effectiveness of using the TRM to retrofit masonry-infilled RC frame buildings with openings, in order to facilitate the use of TRM as a regular method for retrofitting existing buildings in practicing engineering. This is achieved by performing a parametric study on a validated 2D numerical model of a three-story masonry-infilled RC frame with and without TRM considering different size of central openings ranging from 5% to 27%. This parametric study aims to examine (i) the influence of central openings on the lateral response of masonry-infilled RC frames subjected to cyclic loading and (ii) the lateral response of the three-story masonry-infilled RC frame with central openings retrofitted with TRM under cyclic loading. A numerical sensitivity analysis is also performed aiming to investigate the influence of (i) the TRM reinforcement ratio and (ii) the type of mortar used for binding the textile reinforcement on the lateral response of the three-story masonry-infilled RC frame retrofitted with TRM subjected to cyclic loading. The three-story masonry-infilled RC frame model without and with TRM used in this study is validated since the results obtained from these numerical models show acceptable degree of accuracy compared to those obtained from the experimental test at global and local level. Furthermore, the unretrofitted three-story masonry-infilled RC frame model with central opening ranging from 5% to 27% is also validated since the results obtained from the current study presented good correlation to those obtained from past studies. Thus, the three-story masonry-infilled RC frame model without opening and with central opening ranging from 5% to 27% used in this parametric study can predict the real response of such type of structure subjected to in-plane cyclic loading with good accuracy.

For the purpose of this study, the degree of accuracy of the proposed numerical model of a three-story masonry-infilled RC frame with central opening ranging from 5% to 27% is considered acceptable, and therefore the following important findings are derived from the current study regarding the influence of different size of central openings on the in-plane response of masonry-infilled RC frames subjected to cyclic loading:

- The presence of central window openings ranging from 8% to 27% on the masonry-infilled RC frame leads to a decrease in the lateral strength, stiffness, and dissipated energy of the infilled frame by about 10% to 60%. This decrease is more pronounced during the early stages of lateral loading compared to that during the last cycles of loading, which occur at large displacements, due to the brittle nature of the infill wall with opening and its stiffness degradation, which leads to brittle shear failures on RC frames from an early stage of lateral loading due to the presence of the opening.
- The failure modes of the infilled frame with a central opening ranging from 5% to 27% during the cyclic loading include firstly, the corner crushing, diagonal cracking, and sliding shear of the infill wall, and then the frame failure mode which consists of the failure of column-beam joints, and of the shear failure of the columns (short-column mechanism) leading to the development of the soft-story mechanism at the first floor. These failures are more pronounced in the cases where the opening is large (12–27%).

- The new reduction factor of the stiffness of the infill wall due to the presence of central openings which is proposed in this study can be used with an equivalent strut model, which is a macro-model for everyday practice, for simulating masonry-infilled frames with central openings along the diagonal. In that case, the masonry infill wall with openings, could be better represented by multi-diagonal no-tension strut elements instead of a single-diagonal strut element.

From the parametric study regarding the effect of TRM on the in-plane response of masonry-infilled RC frame with central opening subjected to cyclic loading the following conclusions are obtained:

- The TRM increases the lateral strength, global stiffness, and dissipated energy of the masonry-infilled RC frame with central openings varying from 5% to 27% by about 30–100%. The TRM, even in the case of a very large opening, contributes to the increase of the global stiffness and the dissipated energy of the infilled frame with openings, since it provides larger global stiffness and dissipated energy than those of the unretrofitted infilled frame without opening. Adding to this, the TRM delays the strength and the stiffness degradation of the infilled frame due to the presence of the opening leading to a more ductile behavior. The increase in the lateral capacity of the infilled frame with any opening percentage due to TRM is more pronounced during the early stages of lateral loading compared to that during the last cycles of loading, which occur at large displacements.
- TRM contributes to delaying the corner crushing and the diagonal cracking of the infill wall since the shear stresses in retrofitted infilled frames with any opening percentage are more evenly distributed on the infilled frames and they are less localized at the corners of the opening than the ones of the unretrofitted ones.
- The TRM contributes to delaying or even preventing the brittle failures such as short-column mechanism and the soft-story mechanism in the cases when the opening area ranges from 5% to 27% since it contributes to a better distribution of the shear forces and stresses along the height of the structure by even preventing the large shear deformation of the infilled frame due to the presence of large opening.
- The new reduction factor of the stiffness of the TRM-retrofitted infill wall due to the presence of central openings which is proposed in this study can be used for simulating the TRM-retrofitted masonry-infilled RC frames with central openings along the diagonal of the infill wall following the macro-modeling approach. In that case the retrofitted infill wall with openings, could be better represented as a pair of alternatively activated multi-diagonal no-tension strut elements and tension tie elements (tension diagonal) instead of a single-diagonal strut and tie element.

From the sensitivity analysis performed regarding the effect of the TRM reinforcement ratio on the lateral response of the three-story masonry-infilled RC frame retrofitted with TRM the following conclusions are obtained:

- The TRM reinforcement ratio influences the effectiveness of using the TRM composite for retrofitting infilled frames, since by increasing the reinforcement ratio, the lateral capacity of infilled frames is increased leading to a more ductile performance, but this increase is not proportional to the increase of the reinforcement ratio. For example, the lateral strength, stiffness, and dissipated energy of the infilled frame receiving TRM with 3.2% textile reinforcement ratio are increased by about 15–25% compared to the corresponding ones of the infilled frame receiving TRM with 1.3% textile reinforcement ratio.
- In the case of a multi-story infilled frame building, it is important to apply more layers of TRM at its first floor, compared to that applied to the upper stories of the building, in order to increase its lateral capacity by delaying or even preventing brittle failures that usually occur at the first floor (soft-story mechanism) and obtaining a better shear distribution along the height of the structure. For example, in the case of the three-story masonry-infilled frame, examined in this study, its lateral capacity is increased by 15–20% when using three-layers of TRM at the first floor and one layer of TRM at the second floor, compared to the case of using two layers of TRM at the first floor and one layer of TRM at the second floor. This increase is not proportional to the increase of the reinforcement ratio. Furthermore, the global stiffness and the dissipated energy of the three-story masonry-infilled frame with TRM are increased by about 25%-45% and 32%-50%, respectively, in the case of using three layers of TRM with small spacing between the yarns of the textile at the first floor compared to the case of using three layers of TRM with large spacing between the yarns of the textile.

From the sensitivity analysis performed regarding the effect of the type of mortar used for TRM on the lateral response of the three-story masonry-infilled RC frame retrofitted with TRM the following conclusions are obtained:

- The lateral capacity of the infilled frame retrofitted with TRM is increased by about 10% in the case of using mortars for TRM which belong to the R3 class, instead of low-strength mortars, R2 class.
- The use of high-strength mortars for the TRM, especially R4 class of mortar compressive strength > 45 MPa and tensile strength > 4 MPa), results in higher lateral strength, global stiffness and dissipated energy of the three-story masonry-infilled RC frame retrofitted with TRM by about 10%-30% instead of using TRM with relatively low strengths (R2 and R3 class of mortar). This increase is not proportional to that of the mortar mechanical properties, since using mortar with double tensile or compressive strength does not provide double lateral capacity of the retrofitted infilled frame.
- The contribution of the compressive strength of the mortar used for TRM to increase the lateral capacity of infilled frame subjected to cyclic loading is more pronounced compared to that of the tensile strength of mortar used for TRM during the first cycles of loading, since the compressive capacity of TRM contributes to enhance the compression strut of the infill wall, while as the lateral loading increases, the contribution of the tensile capacity TRM to increase the lateral capacity of retrofitted infilled frame becomes more pronounced than the compressive capacity of the TRM since at this stage this composite material sustains the high tensile stresses which are transferred from infill wall to the TRM at local level.

Therefore, there is no doubt that the TRM significantly improves the lateral response of masonry-infilled RC frames with openings subjected to lateral loading by increasing the lateral capacity, stiffness, and the dissipated energy of infilled frames with openings. The TRM leads to a more ductile behavior of infilled frames with openings by delaying the strength and the stiffness degradation of infilled frames due to openings, and further by delaying or even preventing brittle failures and large shear deformations that occur on infilled frames due to the presence of the opening. In the case of using the TRM for seismic retrofitting infilled frames with openings, there is a tendency that the efficiency of TRM at early lateral loading stage is higher than in the case of solid infilled frames, proving the TRM as a suitable method for the in-plane enhancement of masonry-infilled RC frame buildings with openings. Furthermore, the TRM reinforcement ratio and the type of the mortar used for binding the textile reinforcement influence the effectiveness of using the TRM composite for retrofitting infilled frames, since by increasing the reinforcement ratio, or by using high-strength mortars for binding the textile reinforcement, the lateral capacity of infilled frames is increased leading to a more ductile behavior, but this increase is not proportional to the increase of the reinforcement ratio or to the increase of the mechanical properties of the mortar.

The assessment of using the TRM for seismic retrofitting infilled frames with openings as derived from the current study is far from complete due to the lack of experimental data, and therefore, more experimental and numerical research is required to assess the use of TRM for retrofitting masonry-infilled RC frames considering different opening configurations, such as for unsymmetrical window and door openings of different sizes and locations. Although in this study the influence of the number of TRM layers, and the type of inorganic-matrix used for binding the textile reinforcement on the lateral response of infilled frame is investigated numerically, experimental tests are required to study all the possible critical parameters able to affect the efficiency of using the TRM for seismic retrofitting of infilled frames. Thus, future research would be essential to characterize the seismic behavior of infilled frames with and without openings retrofitted with TRM by performing experimental or numerical tests. The expansion of the experimental database is required to study in more depth (a) the effect of using different type of connectors for anchoring the TRM to the bounding RC frame and for anchoring the TRM along the perimeter of the openings, (b) the influence of extending the retrofitting layers applied to infill walls to the faces of the columns and the beams by using different length of overlapping of the textile reinforcement along the infill-frame transition, (c) the influence of using different TRM composites including the textile orientations, the TRM layout by means of using diagonal band of TRM by varying its width, the reinforcement ratio, and (d) the out-of-plane behavior and its interaction with the in-plane behavior of this structural system. Future work in this field should be directed at establishing design guidelines in which the design and detailing using this strengthening solution is achieved in the context of current design formulations to facilitate the implementation of this composite material as a regular method for retrofitting existing buildings.

ACKNOWLEDGMENT

This research did not receive any specific grant from funding agencies in the public, commercial, or not-forprofit sectors.

CONFLICT OF INTEREST

No.

DATA AVAILABILITY STATEMENT

The data are available on request from the authors. The data that supporting the findings of this study are available from the corresponding author upon reasonable request.

ORCID

Filippou Christiana A https://orcid.org/0000-0003-2798-8998

REFERENCES

1. Syrmakezis C, Asteris P. Influence of infilled walls with openings to the seismic response of plane frames. Proc 9th Can Masonry Symp. 2001.
2. Asteris PG. Lateral Stiffness of Brick Masonry Infilled Plane Frames. *J Struct Eng*. 2003;129(8):1071. doi:10.1061/~ASCE!0733-9445~2003!129:8~1071!
3. Chiou YJ, Tzeng JC, Liou YW. Experimental and Analytical Study of Masonry Infilled Frames. *ASCE J Struct Eng*. 1999;125(10):1109-1117.
4. Merhabi A, Shing B, Sculler P, Noland J. Experimental evaluation of masonry-infilled RC frame. *ASCE*. 1996;122(3):228-237.
5. Crisafulli FJ. *Seismic behaviour of reinforced concrete structures with masonry infills*. University of Canterbure New Zeland; 1997.
6. Shing PB, Mehrabi AB. Behaviour and analysis of masonry-infilled frames. *Prog Struct Mater Eng*. 2002;4:320-331. doi:10.1002/pse.122
7. El-Dakhakhni W, Elgaaly M, Hamid A. Three-Strut Model for Concrete Masonry-Infilled Steel Frames. *J Struct Eng*. 2003;129(2):177-185.
8. Asteris PG, Kakaletsis DJ, Chrysostomou CZ, Smyrou EE. Failure modes of in-filled frames. *Elect J Struc Eng*. 2011;11(March 2016):11-20.
9. Chrysostomou CZ, Asteris PG. On the in-plane properties and capacities of infilled frames. *Eng Struct*. 2012;41:385-402. doi:10.1016/j.engstruct.2012.03.057
10. Liauw TC. Tests on Multistory Infilled Frames Subject to Dynamic Lateral Loading. *ACI J Proc*. 1979;76(4):551-564.
11. Liauw and Kwan. Nonlinear behaviour of non-integral infilled frames. *Proc Inst Civ Eng* 1983; 18(3): 551-560.
12. Liauw and Kwan. Non-linear analysis of infilled frames. 1984; 6: 223-231.
13. Mehrabi A, Benson Shing P, Schuller M, Noland J. Experimental Evaluation of Masonry-Infilled RC Frames. *J Struct Eng*. 1996;122(3):228-237.
14. Mosalam KM, Richard W, Gergely P. Static response on infilled frames using quasi-static experimentation. *ASCE J Struct Eng*. 1997;123(11):1462-4169.
15. Zarnic R, Tomazevic M. *An experimentally obtained method for evaluation of the behavior of masonry infilled R/C frames*. 1988.
16. Mehrabi A, Shing PB, Schuller M, Noland J, Performance of masonry-infilled R/C frames under in-plane lateral loads. 1994.
17. Buonopane SG, White RN. Pseudodynamic Testing of Masonry Infilled Reinforced. *J Struct Eng*. 1999;125(6):578-589. doi:10.1061/(ASCE)0733-9445(1999)125:6(578)
18. Stavridis A, Shing PB. Finite-element modeling of nonlinear behavior of masonry-infilled RC frames. *J Struct Eng*. 2010;136(3):285-296. doi:10.1061/(ASCE)ST.1943-541X.116
19. Basha SH, Kaushik HB. Behavior and failure mechanisms of masonry-infilled RC frames (in low-rise buildings) subject to lateral loading. *Eng Struct*. 2016;111:233-245. doi:10.1016/j.engstruct.2015.12.034
20. Singhal Vaibhav, ‡, Durgesh C, Rai. In-plane and out-of-plane behavior of confined masonry walls for various toothing and openings details and prediction of their strength and stiffness. *Earthquake Eng Struct Dyn*. 2016(45):2551-2569. doi:10.1002/eqe.2783
21. Parisi Fulvio, *, NAD. Seismic capacity of irregular unreinforced masonry walls with openings. *Earthquake Eng Struct Dyn*. 2013(42):101-121. doi:10.1002/eqe.2195. Seismic.
22. Akhoundi Farhad, *, † PBL and GV. Numerically based proposals for the stiffness and strength of masonry infills with openings in reinforced concrete framES. *Earthquake Eng Struct Dyn*. 2016(45):869-891. doi:10.1002/eqe.2688
23. Mansouri A, Marefat MS, Khanmohammadi M. Analytical estimation of lateral resistance of low-shear strength masonry infilled reinforced concrete frames with openings. *Struct Des Tall Special Build*. 2018;27(6):1-13. doi:10.1002/tal.1452
24. Mallick DVGR. Effect of openings on the lateral stiffness of infilled frames. *Civil Eng*. 1971;49:193-201.
25. Kakaletsis DJ, Karayannis CG. Influence of masonry strength and openings on infilled R/C frames under cycling loading. *J Earthquake Eng*. 2008;12(2):197-221. doi:10.1080/13632460701299138
26. Kakaletsis D, Karayannis C. Experimental investigation of infilled r/c frames with eccentric openings. *Struct Eng Mech*. 2007;26(3):231-250. doi:10.12989/sem.2007.26.3.231
27. Kakaletsis DJ, Karayannis CG. Experimental investigation of infilled reinforced concrete frames with openings. *ACI Struc J*. 2009;106(2):132-141.
28. Mallick DV, Garg RP. Effect of openings on the lateral stiffness of infilled frames. *Proc Inst Civ Eng*. 1971;49(19).
29. Liauw TC. Tests on Multistory Infilled Frames Subject to Dynamic Lateral Loading. *Proc Inst Civ Eng*. 1979;76(4):551-564.
30. Utku B. *Stress magnification in walls with opoenigs*. 1980.
31. Dawe JLYT. *An Investigation of Factors Influencing the Behaviour of Masonry Infill*. 1985.
32. Asteris PG, Giannopoulos IP, Chrysostomou CZ. Modeling of Infilled Frames With Openings. *Open Constru Build Technol J*. 2012;6(6):81-91.
33. Buonopane SG, White RN. Pseudodynamic Testing of Masonry Infilled Reinforced. *J Struct Eng*. 1999;125(6):578-589. doi:10.1061/(ASCE)0733-9445(1999)125:6(578)
34. Chiou YJ, Tzeng JC, Liou YW. Experimental and analytical study of masonry infilled frames. *J Struct Eng*. 1999;125(10):1109-1117.

35. Decanini L, Liberatore L, Mollaioli F, The influence of openings on the seismic behaviour of infilled framed structures. *Conference: 15th World Conference on Earthquake Engineering* 2012 2014.
36. De Luca F, Verderame GM, Gómez-Martínez F, Pérez-García A. The structural role played by masonry infills on RC building performances after the 2011 Lorca, Spain, earthquake. *Bull Earthquake Eng*. 2014;12(5):1999-2026. doi:10.1007/s10518-013-9500-1
37. Hermanns L, Fraile A, Alarcón E, Álvarez R. Performance of buildings with masonry infill walls during the 2011 Lorca earthquake. *Bull Earthquake Eng*. 2014;12(5):1977-1997. doi:10.1007/s10518-013-9499-3
38. Tondelli, Beyer1 Katrin, * † and Matthew DeJong2 1Earthquake. Influence of boundary conditions on the out-of-plane response of brick masonry walls in buildings with RC slabs. *Earthquake Eng Struct Dynamics*. 2016(45):13374-11356. doi:10.1002/eqe
39. Di Domenico M, Ricci P, Verderame GM. Experimental Assessment of the Influence of Boundary Conditions on the Out-of-Plane Response of Unreinforced Masonry Infill Walls. *J Earthquake Eng*. 2020;24(6):881-919. doi:10.1080/13632469.2018.1453411
40. Furtado A, Rodrigues H, Arêde A, Varum H. Experimental evaluation of out-of-plane capacity of masonry infill walls. *Eng Struct*. 2016;111:48-63. doi:10.1016/j.engstruct.2015.12.013
41. Ricci P, Domenico M, Verderame GM. Experimental assessment of the in-plane/out-of-plane interaction in unreinforced masonry infill walls. *Eng Struct*. 2018;173:960-978. doi:10.1016/j.engstruct.2018.07.033
42. Triantafillo. Strengthening of masonry structures using epoxy-bonded FRP laminates. *ASCE J Struct Eng*. 1998:104-111.
43. Albert ML, Elwi AE, and CJJ. Strengthening of Unreinforced Masonry Walls Using FRPs. *ASCE J Composites for Const*. 2001;5:76-84.
44. Almusallam TH, Al-Salloum YA. Behavior of FRP Strengthened Infilled Walls Under In-Plane Seismic Loading. *ASCE J Composites for Const*. 2007;11:308-318.
45. Akhoundi F, Lourenço PB, Vasconcelos G, Numerical modelling of masonry-infilled reinforced concrete frames : Model calibration and parametric study 2014: 1-13.
46. Kim YY, Kong HJ, and VCL. Design of Engineered Cementitious Composite Suitable for Wet-Mixture Shotcreting. *ACI Mater J*. 2003;100(6):511-518.
47. Kyriakides MA, Billington SL, Seismic Retrofit Of Masonry-Infilled Non-Ductile Reinforced Concrete Frames Using Sprayable Ductile Fiber-Reinforced Cementitious Composites. *The 14 World Conference on Earthquake Engineering* 2008.
48. Akhoundi F, Vasconcelos G, Lourenço P, Silva LM, Cunha F, Fangueiro R. In-plane behavior of cavity masonry infills and strengthening with textile reinforced mortar. *Eng Struct*. 2018;156(November 2017):145-160. doi:10.1016/j.engstruct.2017.11.002
49. Koutas L, Triantafillou T, Bousias S. Seismic Strengthening of Masonry-Infilled RC Frames with TRM: experimental Study. *J Compos Constr*. 2014;19(2):04014048. doi:10.1061/(ASCE)CC.1943-5614.0000507
50. Parisi F, Iovinella I, Balsamo A, Augenti N, Prota A. In-plane behaviour of tuff masonry strengthened with inorganic matrix-grid composites. *Composites Part B: Engineering*. 2013;45(1):1657-1666. doi:10.1016/j.compositesb.2012.09.068
51. Filippou CA, Kyriakides NC, Chrysostomou CZ. Numerical Modelling and Simulation of the In-Plane Response of a Three-Storey Masonry-Infilled RC Frame Retrofitted with TRM. *Adv Civil Eng*. 2020;2020:1-19. doi:10.1155/2020/6279049
52. Filippou C, Furtado A, De Risi MT, Kyriakides N, Chrysostomou CZ. Behaviour of Masonry-Infilled RC Frames Strengthened Using Textile Reinforced Mortar: an Experimental and Numerical Studies Overview. *J Earthquake Eng*. 2022;26(00):7743-7767. doi:10.1080/13632469.2021.1988763
53. Benedetti D, Carydis P, Pezzoli P. Shaking table tests on 24 simple masonry buildings. *Earthquake Eng Struct Dyn*. 1998;27(1):67-90. doi:10.1002/(SICI)1096-9845(199801)27:1<67::AID-EQE719>3.0.CO;2-K
54. Colombo A, Negro P, Verzeletti G. *Improving Ductility and Energy-Dissipation Capacity of Infills By Means of Polymeric Nets*. 2000:1-7.
55. Kalali A, Kabir MZ. Cyclic behavior of perforated masonry walls strengthened with glass fiber reinforced polymers. *Scientia Iranica*. 2012;19(2):151-165. doi:10.1016/j.scient.2012.02.011
56. Triller P, Tomaževič M, Gams M. Seismic behaviour of multistorey plain masonry shear walls with openings: an experimental study. *Brick and Block Masonry*. 2016:1949-1954. doi:10.1201/b21889-256
57. Be GuJ, n, Y Tao, Xin R, Yang Z, Shi QX. Seismic Performance of Multistorey Masonry Structure with Openings Repaired with CFRP Grid. *Adv Civil Eng*. 2018;2018:1-11. doi:10.1155/2018/4374876
58. Mohan A, Jacob B, Strength and Ductility in unreinforced masonry walls with two openings retrofitted by Carbon Fiber Reinforced Polymers 2016: 346-352.
59. Proença JM, Gago AS. Vilas Boas A. Structural window frame for in-plane seismic strengthening of masonry wall buildings. *Int J Architectural Heritage*. 2019;13(1):98-113. doi:10.1080/15583058.2018.1497234
60. da Porto F, Guidi G, Verlato N, Modena C. Effectiveness of plasters and textile reinforced mortars for strengthening clay masonry infill walls subjected to combined in-plane/out-of-plane actions /Wirksamkeit von Putz und textilbewehrtem Mörtel bei der Verstärkung von Ausfachungswänden aus Ziegel. *Eur J Masonry*. 2015;19(5):334-354. doi:10.1002/dama.201500673
61. Koutas L, Triantafillou T, Bousias S. Analytical Modeling of Masonry-Infilled RC Frames Retrofitted with Textile-Reinforced Mortar. *J Compos Constr*. 2014;19(5):1-14. doi:10.1061/(ASCE)CC.1943-5614.0000553
62. Ismail N, El-maaddawy T, Khattak N. Quasi-static in-plane testing of FRCM strengthened non-ductile reinforced concrete frames with masonry infills. *Constr Build Mater*. 2018;186:1286-1298. doi:10.1016/j.conbuildmat.2018.07.230
63. Sagar S, Singhal V, Durgesh C, Rai M. In-Plane and Out-of-Plane Behavior of Masonry-Infilled RC Frames Strengthened with Fabric-Reinforced Cementitious Matrix. *ASCE J Struct Eng*. 2019;23(1).
64. Fillippou CA, Chrysostomou CZ, Kyriakides N. Effect of the TRM reinforcement ratio on the lateral response of a three-story masonry-infilled RC frame retrofitted with TRM. *fib Symposium 2021 Concrete Structures: New Trends for Eco-Efficiency and Performance*. 2021.
65. BSI. Eurocode 2 : Design of concrete structures — Part 1.2 General rules — Structural fire design 2003.

66. TNO DIANA. DIANA FEA version 10.2.
67. Filippou CA, Numerical study on the seismic retrofitting of masonry-infilled RC frames using textile-reinforced mortar. 2021.
68. Filippou CA, Kyriakides NC, Chrysostomou CZ. Numerical Modeling of Masonry-infilled RC Frame. *The Open Construction and Building Technol J*. 2019;13(1):3-16. doi:10.2174/1874836801913O1
69. Filippou C, Kyriakides N, Chrysostomou CZ. EFFECT OF CONNECTION DETAIL AT INTERFACE OF MASONRY- INFILLED RC FRAMES RETROFITTED WITH TRM. *17th World Conference on Earthquake Engineering, 17WCEE Sendai*. 2020:2020. *Japan - September 13th to 18th*.
70. Filippou C, Chrysostomou C, Kyriakides N, Numerical Modeling of Masonry-Infilled Rc Frame Strengthened With Trm. *7th ECCOMAS Thematic Conference on Computational Methods in Structural Dynamics and Earthquake Engineering*, 2019. doi:10.7712/120119.7136.19665
71. Filippou CA, Chrysostomou CZ. Analytical model for textile reinforced mortar under monotonic loading. *Constr Build Mater*. 2020;258:120178. doi:10.1016/j.conbuildmat.2020.120178
72. Tekeli H, Aydin A. An experimental study of the seismic behavior of Infilled RC frames with opening. *Scientia Iranica*. 2017;24(5):2271-2282. doi:10.2420/sci.2017.4150
73. Akhoundi F, Lourenço PB, Vasconcelos G. Numerically based proposals for the stiffness and strength of masonry in fi lls with openings in reinforced concrete frames. *Earthquake Eng Struct Dynamics*. 2016;45(2):869-891. doi:10.1002/eqe.2688
74. Ahani E, Mousavi MN, Rafezy B, Osmanzadeh F. Effects of Central Opening in Masonry Infill on Lateral Behavior of Intermediate RC Frames. *Advances in Civil Eng Materials*. 2019;8(1):20180040. doi:10.1520/acem20180040
75. Liauw TC. An Approximate Method of Analysis for Infilled Frames with or without Opening. *Build Sci*. 1972;7(7):233-238.
76. Fiorato AE, Sozen MA, Gamble WL. *An Investigation of the Interaction of Reinforced Concrete Frames with Masonry Filler Walls*. Dept of Civil Engineering, University of Illinois; 1970:70-100. *Report No UILU-ENG-*.
77. Mosalam KM, White RN, Gergely P, Seismic Evaluation of Frames with Infill Walls Using Pseudo-dynamic Experiments. 1997.
78. Morandi P, Hak S, Magenes G. Performance-based interpretation of in-plane cyclic tests on RC frames with strong masonry infills. *Eng Struct*. 2018;156(November 2017):503-521. doi:10.1016/j.engstruct.2017.11.058
79. Asteris PG, Chrysostomou CZ, Giannopoulos IP, Smyrou E, Masonry Infilled Reinforced Concrete Frames With. *III ECCOMAS Thematic Conference on Computational Methods in Structural Dynamics and Earthquake Engineering* 2011.
80. Surendran S, Kaushik H. Masonry infill RC frames with openings: review of in-plane lateral load behaviour and modeling approaches. *Open Constr Build Technol J*. 2012;6:126-154. doi:10.2174/1874836801206010126
81. Cetisli F. Effect of openings on infilled frame stiffness. *Gradjevinar*. 2015;67(8):787-797. doi:10.14256/JCE.1155.2014
82. Stafford-Smith B. Methods for predicting the lateral stiffness and strength of multi-storey infilled frames. *Build Sci*. 1967;2(3):247-257. doi:10.1016/0007-3628(67)90027-8
83. Mainstone RJ. Supplementary note on the stiffness and strength of infilled frames. *Building Res*. 1974.
84. Bazān E, Meli R. Seismic Analysis of Structures Hth Masonry Walls. *IitkAcIn*. 1980.
85. Crisafulli FJ, Carr AJ. Proposed macro-model for the analysis of infilled frame structures. *Bulletin of the New Zealand Society for Earthquake Eng*. 2007;40(2):69-77.
86. FEMA 306. *Evaluation of earthquake damaged concrete and masonry wall buildings*. FEMA, 1998.
87. Thiruvengada. On the natural frequencies of infilled frames. *Earthquake Eng Struct Dyn*. 1985:401-419.
88. Chrysostomou CZ. Effects of degrading infill walls on the nonlinear seismic response of two-dimensional steel frames. *Dissertation Abstracts Intl*. 1991;51(12):348.
89. El-Dakhakhni WW, Elgaaly M, Hamid AA. Finite Element Modeling of Concrete Masonry-Infilled Steel Frame. *9th Canadian Masonry Symposium*. 2001.
90. El-Dakhakhni. Experimental and Analytical Seismic Evaluation of Concrete Masonry-Infilled Steel Frames Retrofitted using GFRP Laminates. 2002.
91. El-Dakhakhni WW, Hamid AA, Elgaaly M, Strength and Stiffness Prediction of Masonry Infill Panels. *13th World Conference on Earthquake Engineering* 2004;3089.
92. Koutas LN, Bournas DA. Out-of-Plane Strengthening of Masonry-Infilled RC Frames with Textile-Reinforced Mortar Jackets. *J Compos Constr*. 2018;23(1):04018079. doi:10.1061/(asce)cc.1943-5614.0000911
93. Pohoryles DA, Bournas DA. A unified macro-modelling approach for masonry-infilled RC frames strengthened with composite materials. *Eng Struct*. 2020;223(June):111161. doi:10.1016/j.engstruct.2020.111161
94. EN 1504-3. *Products and systems for the protection and repair of concrete structures. Definitions, requirements, quality control and evaluation of conformity*. Part 3: Struct and Non-Structural Repair. 2006.

How to cite this article: A FC, Kyriakides NC, Chrysostomou CZ. Numerical study of the seismic retrofitting of masonry-Infilled RC frames with openings using TRM. *Earthquake Engng Struct Dyn*. 2023;52:776–805. https://doi.org/10.1002/eqe.3787